HHS Public Access

Author manuscript

Hear Res. Author manuscript; available in PMC 2022 May 01.

Published in final edited form as:

Hear Res. 2021 May ; 404: 108216. doi:10.1016/j.heares.2021.108216.

Development of a chronically-implanted mouse model for studies of cochlear health and implant function.

Deborah J. Colesa, **Jenna Devare**, **Donald L. Swiderski**, **Lisa A. Beyer**, **Yehoash Raphael**, **Bryan E. Pfingst**

Kresge Hearing Research Institute, Department of Otolaryngology - Head and Neck Surgery, University of Michigan, Ann Arbor, MI, USA

Abstract

Mice with chronic cochlear implants can significantly contribute to our understanding of the relationship between cochlear health and implant function because of the availability of molecular tools for controlling conditions in the cochlea and transgenic lines modeling human disease. To date, research in implanted mice has mainly consisted of short-term studies, but since there are large changes in implant function following implant insertion trauma, and subsequent recovery in many cases, longer-term studies are needed to evaluate function and perception under stable conditions. Because frequent anesthetic administration can be especially problematic in mice, a chronic model that can be tested in the awake condition is desirable. Electrically-evoked compound action potentials (ECAPs) recorded with multichannel cochlear implants are useful functional measures because they can be obtained daily without anesthesia. In this study, we assessed changes and stability of ECAPs, electrically-evoked auditory brainstem responses (EABRs), ensemble spontaneous activity (ESA), and impedance data over time after implanting mice with multichannel implants. We then compared these data to histological findings in these implanted cochleae, and compared results from this chronic mouse model to data previously obtained in a well-established chronically-implanted guinea pig model. We determined that mice can be chronically implanted with cochlear implants, and ECAP recordings can be obtained frequently in an awake state for up to at least 42 days after implantation. These recordings can effectively monitor changes or stability in cochlear function over time. ECAP and EABR amplitude-growth functions (AGFs), AGF slopes, ESA levels and impedances in mice with multichannel implants appear similar to those found in guinea pigs with long-term multichannel implants. Animals with better survival of spiral ganglion neurons (SGNs) and inner hair cells (IHCs) have steeper AGF slopes, and larger ESA responses. The time course of post-surgical ear

Address correspondence to: Bryan E. Pfingst, Ph.D., Kresge Hearing Research Institute, 1150 West Medical Center Drive, Ann Arbor, MI 48109-5616, bpfingst@umich.edu, Phone: 734-763-2292.

Author Statement

The data from our mouse experiments presented in this manuscript are original and have not been submitted for publication elsewhere. All authors have contributed to this work and have approved the manuscript, its content, and its submission to Hearing Research. All authors declare that they have no conflict of interest.

Conflict of Interest Disclosure Statement

The authors declare no COI.

recovery may be quicker in mice and can show different patterns of recovery which seem to be dependent on the degree of insertion trauma and subsequent histological conditions. Histology showed varying degrees of cochlear damage with fibrosis present in all implanted mouse ears and small amounts of new bone in a few ears. Impedance changes over time varied within and across animals and may represent changes over time in multiple variables in the cochlear environment post-implantation. Due to the small size of the mouse, susceptibility to stress, and the higher potential for implant failure, chronic implantation in mice can be challenging, but overall is feasible and useful for cochlear implant research.

Keywords

auditory prosthesis; mouse; electrically-evoked compound action potential (ECAP); cochlear implant

1. Introduction

Cochlear implants function by stimulating auditory neurons using an array of electrodes placed in the cochlea. It is therefore not surprising that the function of the implant, including its ability to deliver patterned stimulation that can be recognized as speech, is influenced by the health of the auditory nerve and any surviving hair cells, and by the tissues that surround the implant in the cochlea. We refer to this overall cochlear condition as cochlear health, which is assessed using histological samples evaluated with light microscopy. Most of the work to date relating cochlear health in the implanted cochlea to cochlear implant function has utilized monkey, cat, rat, and guinea pig animal models. However, several attempts have been made to develop a cochlear-implanted mouse model. A mouse as a model offers some significant advantages for studying the relationship between cochlear pathology and cochlear implant function because of the availability of well-developed genetic technologies allowing the control of specific biological tissues. One example is the diphtheria-toxin-receptor (DTR) mouse in which all hair cells can be destroyed while leaving the auditory nerve intact for at least two months (Tong et al., 2015; Kurioka et al., 2016), a condition that is not currently available in other animal models. Another advantage of an implanted-mouse model is the availability of genetically-altered animals that mimic human cochlear pathologies, as summarized in a recent review (Ohlemiller et al., 2016).

Previous studies have shown that placing cochlear implants in mice is feasible but can be technically challenging (Irving et al., 2013; Soken et al., 2013, Mistry et al., 2014; Navntoft et al., 2019; Claussen et al., 2019). The small tympanic bulla and cochlea, and the large stapedial artery close to the round window, make implantation an especially delicate procedure and use of a small implant imperative. After implantation, determining safe stimulation ranges, and maintaining a functioning chronic implant over a long term, can be difficult. The goal of the current study was to test and refine the chronically-implanted mouse model with emphasis in particular on monitoring the effects of implant insertion and stimulation over time post implantation on the anatomy and the function of the implanted ear. Understanding the response of a normal cochlea to implant insertion and use is

prerequisite to using animal models for understanding the function of the implant in pathological or genetically modified ears.

Most implant insertions do some physical damage to the cochlea and/or cause inflammation and tissue growth (Kamakura and Nadol, 2016; Okayasu et al., 2020), potentially impacting the short and long-term health of the cochlea and the function of the implant. Therefore, in developing a mouse model to study effects of cochlear pathology, it is important to determine what effects the implant surgery itself has on conditions in the implanted cochlea. In this study, as in previous studies in guinea pigs (Kang et al., 2010; Pfingst et al., 2017; Swiderski et al., 2020; Schvartz-Leyzac et al., 2020), we used three histological measures, assessed with light microscopy, to determine anatomical effects of inserting and stimulating a cochlear implant in a normal ear: spiral ganglion neuron (SGN) density; inner hair cell (IHC) survival; and tissue growth (fibrosis and neo-osteogenesis) in the scala tympani.

The functional response of the cochlea to the trauma caused by cochlear implant insertion and stimulation is not a one-and-done event, but rather a complex, ongoing process lasting weeks or months. In previous studies of cochlear implants in nonhuman primates and in guinea pigs, we found that functional responses to electrical stimulation are highly variable and generally poor during the first days or weeks after implantation, and then eventually improve and reach a long-term-stable level that reflects long-term cochlear health and function (Pfingst, 1990; Su et al., 2008; Pfingst et al., 2015; Schvartz-Leyzac et al., 2019). Therefore, our first priorities in developing a useful mouse model were to determine the nature and extent of damage caused by surgical insertion of the implant and determine time course of changes in functional responses following implantation. Monitoring the reduction and recovery of function over time after implantation requires repeated functional measurements over time, especially in the days and weeks following implantation. A useful functional measure for this purpose is the electrically-evoked compound action potential (ECAP) amplitude-growth function (AGF) recorded from one of the electrodes in the cochlea in response to stimulation of an adjacent electrode. In cochlear-implanted guinea pigs, slopes of these functions (i.e., the rate at which the ECAP amplitude grows as a function of stimulus current level) have been shown to correlate with the health of the implanted cochlea as assessed anatomically: specifically, SGN density and IHC survival near the electrodes (Pfingst et al., 2017). Other, related ECAP measures are also predictive of cochlear neural health (Prado-Guitierrez et al., 2006; Ramekers et al., 2014). In cochlear-implanted humans, several of these ECAP measures have been shown to be predictive of speech recognition (Kim et al., 2010; DeVries et al., 2016; Schvartz-Leyzac and Pfingst, 2018). In guinea pigs the slopes of these functions typically decrease over the first few days following implantation and then increase over the following weeks eventually reaching a stable level where they reflect the degree of SGN density and IHC survival (Pfingst et al., 2015; Schvartz-Leyzac et al., 2019). When using a mouse model to understand the relationship between cochlear health and implant function, it is important to understand the time course of changes in functional responses to implant insertion and preferably to plan experiments during a period when these functional responses have recovered from insertion trauma and reached long-term stability. The ECAP AGF measure is suitable for the mouse because it is robust and can be recorded daily in awake animals thereby decreasing the risks related to frequent and repeated use of anesthesia, which is often detrimental for long-term

studies. We previously demonstrated that ECAP AGFs were measurable in implanted mice (Colesa et al., 2017; Conference on Implantable Prosthesis) but we measured those functions only once on the day of surgery. In this study, we followed this measure over time after implantation to determine if function improved, stabilized and was related to cochlear health, as we have found in guinea pigs.

Historically, a more frequently used functional measure of the condition of the implanted cochlea has been the electrically evoked auditory brainstem responses (EABR). Like the ECAP, the slopes of the EABR AGFs reflect SGN survival (Smith and Simmons, 1983; Hall, 1990). EABRs can be useful for assessing aspects of cochlear health just as the ECAP, but they require anesthesia, which poses challenges for taking daily measurements in any species but especially mice as daily and repeated doses of anesthesia can be a major risk factor. Since, anesthesia related deaths can impact long-term studies, EABR is not as useful for following early changes over time where rapid changes are expected in a short period of time, but may be more useful for tracking long-term trends, or assessing stability and relationship to cochlear health just prior to study endpoints. Another advantage to using ECAP over EABR is that the recording electrodes are much closer to the auditory nerve, and therefore may more closely reflect cochlear conditions near the site of stimulation. Also, ECAP measures are more commonly used in a clinical setting than EABR. Thus ECAP is the safer and more relevant choice for looking at short and long-changes in cochlear function.

Another useful measure of cochlear health is ensemble spontaneous activity (ESA) (Dolan et al., 1990; Searchfield et al., 2004). ESA measures reflect the spontaneous activity in the ensemble of auditory nerve fibers which is typically dependent on the presence of functioning IHCs. ESA amplitudes presumably are affected by the density of auditory neurons near the recording electrode as well as the amount of spontaneous activity in those fibers. Thus, they provide information about the condition of the IHCs and auditory nerve array that is likely to affect its response to electrical and acoustic stimulation. Also, this measure does not require stimulation and therefore would have less effect on long-term survival if overstimulation was a factor limiting mouse survival after implantation. ESA can be recorded in the awake-condition, but due to noise contamination of the response in awake animals, it is best measured under anesthesia. Daily doses of anesthesia, as mentioned above, are not ideal for long-term studies in mice; therefore, ESA measures performed at more widely spaced time intervals (possibly guided by observed changes in ECAP) throughout long-term studies and at end points would be a useful measure for understanding this aspect of cochlear health.

Electrode impedance was measured daily in this study, primarily to determine the integrity of the implant, monitor wire breakage, etc. Impedance has been associated with the growth of fibrous tissue in the implanted cochlea (Wilk et al., 2016), but several published studies suggest that other physical variables underlie impedance changes overtime (Duan et al., 2004; Su et al., 2008; Newbold et al., 2014; Schvartz-Leyzac et al., 2019).

Finally, to put the research in mice in perspective, we compared the results to previous work from our laboratory that used guinea pigs (Kang et al., 2010; Pfingst et al., 2017; Swiderski et al., 2020; Schvartz-Leyzac et al., 2020).

In summary, the objective of this study was to build on previous work and continue the development of a mouse model for experimental studies of the relationship between cochlear health and cochlear implant function. The emphasis was on a chronic model that can utilize daily monitoring of implant function following implantation to assess the functional effects of implant insertion trauma and the recovery process so that data can be obtained under long-term stable conditions which model those in human cochlear implant users. We monitored cochlear health as defined by well-developed histological variables to determine the short and intermediate-term effects of insertion trauma on cochlear health at the anatomical level and we assessed cochlear implant function over time using electrophysiological and impedance measures. Finally, we compared these results to those from a well-established guinea pig model.

2. Methods

2.1 Overview

Non-deafened adult male wild type (CBA/CaJ Pou4f3 +/+, N = 5, 20-24 g, 1.5 – 1.8 months of age at implantation, 2.3 – 3.2 months of age at euthanasia) mice were implanted in the scala tympani with a multichannel cochlear implant comprised of 3 platinum/iridium electrodes (See Table 1 for subject summary). ECAPs were obtained in the awake condition 8 or 9 days post-implantation (DPI) and measured every 2 to 7 days for up to 42 DPI; electrode impedances were also measured on this schedule. EABRs and ESAs were recorded weekly under anesthesia. Electrophysiology was followed over time to monitor changes in neural function and to determine when recorded activity stabilized. Mouse survival times were not pre-set; rather, factors such as functional longevity of the implants, stability of the percutaneous connector (acrylic, screws, and implant base mounted to the skull), and tolerance to repeated anesthetics and/or stimulation determined end points. At these end points, mice were euthanized and histological analyses were performed to assess SGN densities, IHC presence, and presence of fibrous tissue and/or new bone.

Mice and guinea pigs used in these experiments were bred, housed and maintained in-house by the Unit for Laboratory Animal Medicine at the University of Michigan. The animal-use protocol was reviewed and approved by the Institutional Animal Care and Use Committee.

2.2 Auditory Brainstem Responses

Prior to implantation, mice were tested for normal hearing thresholds using ABRs to verify they did not have any pre-existing ear dysfunction in the left ear that was to be implanted. To measure ABRs, animals were anesthetized with ketamine (120 mg/kg) and xylazine (7 mg/kg) and placed on a heating blanket with an acoustic transducer placed just inside the tragus, directed at the tympanic membrane. Needle electrodes were positioned subcutaneously at the vertex and bilaterally underneath the pinnae. Responses to tone bursts at 8, 20 and 32 kHz were tested.

2.3 Implantation Procedures

Mice were anesthetized with isoflurane and oxygen, and placed on a heating pad. Temperature and oxygen levels were monitored with a rectal temperature probe and pulse oximeter, respectively. Ketoprofen (5 mg/kg) for pain management and glycopyrrolate (0.02 mg/kg) to decrease salivation and improve respiration were administered subcutaneously. The surgery area was shaved, and then scrubbed alternately, 3 times each, with warmed chlorhexidine surgical scrub and 70% isopropyl alcohol. The animal was draped and a skin incision was made behind the left ear. Muscle and connective tissue were dissected to expose the bulla. With a hand drill, the bulla was punctured and the hole made large enough to insert fine forceps for bone removal. Bone was removed to create a defect large enough to visualize the round window membrane. Once the round window was identified and the middle ear space inspected and determined to be normal, the bulla hole was temporarily closed with a piece of cotton. An incision was made on the midline of the skull to expose the bregma. The periosteum was incised and scraped laterally to separate it from the skull. The skull was scrubbed with 3% hydrogen peroxide and flushed with saline. Three screws were inserted into the skull to create a support for the implant base, which was embedded in methyl methacrylate (dental acrylic) and secured to the screws with additional acrylic. The ground ball was placed in the neck muscle above the bulla defect. The bulla defect was then reopened and the implant carefully inserted through the round window membrane into the scala tympani. The round window was then sealed with muscle to prevent excessive perilymph flow and the migration of the implant. Carboxylate cement was used to seal the bulla defect and secure the implant to the bone. In the first three mice implanted, implants were sutured to the muscle at three locations from the acrylic base to the bulla in an “S” like pattern to help hold the implant in place and deter migration out of the cochlea; this was also done to prevent the excess cable from putting extra pressure on the closed incision. After implants broke quickly in the first three mice, implants were left loose in the last two mice to allow the implant to move more freely with the mouse. After securing of the implant, the post-auricular incision was sutured with an absorbable subcutaneous uninterrupted suture and the skin closed with non-absorbable interrupted suture. Additional dental acrylic was applied to the skull, screws and base to completely seal the opening on the skull and hold the base secure (percutaneous connector). Excess skin around the acrylic was trimmed slightly so skin would not be pushed down over the eye or force the pinna into an abnormal position. Loctite adhesive was applied to the surface of the acrylic to seal the small holes that could eventually absorb liquids and soften it.

2.4 Cochlear Implants

The cochlear-implant electrode array (Figure 1) consisted of 3 half-band platinum/iridium electrodes (~ 0.25 mm) embedded in a silicone rubber carrier (Cochlear® HL03 animal array, Sydney, Australia) and a flamed platinum/iridium ground ball (0.8 ±0.15 mm). Electrode spacing on the intracochlear array was approximately 0.45 mm center to center and the diameter of the portion of the implant inserted into the cochlea was 0.15 mm. All electrodes were activated for 5 minutes in a saline bath prior to sterilization for implantation. Insertion depths for the intracochlear electrode array ranged from 1.6 – 2.5 mm (average 2.0 mm) past the round window. The primary electrode used for stimulation was the most apical electrode (electrode 1, Figure 1) which was located an average of 1.5 mm apical to the round

window and was the location at which the cochlea was sectioned for histological assessment. Data were also collected from electrodes 2 and 3 when they were functional and testing was not restricted due to an anesthetic time window. Implants were identified with the mouse number, the ear implanted and number of times the ear was implanted (i.e. 7707L1).

2.5 Histology

After electrophysiological data collection was complete and while mice were still anesthetized, or after accidental death, mice were decapitated and heads were placed in 4% paraformaldehyde. Temporal bones were extracted with the implant remaining in place in the implanted ear. The tissues were decalcified in 3% EDTA for 1 to 2 weeks until the bone was soft. When decalcification was complete and the cochlear-implant electrodes were visible through the bone, the cochleae were marked in the lateral wall at the location of electrode 1. The implant was then gently removed. Tissues were embedded in JB-4 (Electron Microscopy Sciences, Hatfield, PA) and sectioned with glass knives to obtain 3 μm thick sections in a mid-modiolar plane centered at the location of the previously made mark and thus centered at the location of electrode 1. This provided views of three profiles that were labeled “A” through “C” as illustrated in Figure 2.

Approximately 15 sections were collected per cochlea with three chosen for analysis. The first section chosen was a section close to the mark that indicated the location of electrode 1. If that section was damaged, the next closest section was used. Two other sections were then selected at intervals separated by a minimum of 2 sections (~ 6 μm) in order to prevent counting same cell more than once. The mid-modiolar sections used for spiral ganglion neuron (SGN) counts were stained with toluidine blue. The specimens were evaluated with a Leica DMRB epifluorescence microscope (Leica, Eaton, PA) and photographed with a CCD Cooled SPOT-RT digital camera (Diagnostic Instruments, Sterling Heights, MI). The cross-sectional area within Rosenthal’s canal containing SGN cell bodies was determined using ImageJ software, and the cell bodies in each of the 3 selected sections were counted. Density of SGNs was calculated by dividing the number of cells counted by this cross-sectional area. Only cells in which nuclei were round and had a diameter of 6 μm or more were considered. Of these cells, only healthy-appearing cells were counted. Presence of IHCs in each profile was recorded if the stereocilia bundle was present. Examples of the sections of Rosenthal’s canal and the organ of Corti that were assessed are shown in Figures 3 and 4 respectively.

SGN densities presented on graphs are averages across profiles A through C. These profiles were chosen for comparison to the functional data because they represented the region closest to the implant (Profile A) and profiles apical to the implant (Profiles B and C). These regions would be most likely to reflect pathology affecting responses to the cochlear implant stimulation presented when measuring ECAPs and EABRs at supra-threshold levels. IHC survival coded on graphs is representative of survival across Profiles A through C.

The presence of intrascalar tissue and new bone was noted in each histological profile. Intrascalar tissue was rated as either low (some tissue present) or high density (filled the entire scala tympani).

Contralateral ears from all 5 implanted mice were sectioned for a non-implanted comparison. Examples of a “normal” cross-section of Rosenthal’s canal and the organ of Corti are shown in Figures 3d and 4d respectively. For ease of comparison between implanted and non-implanted ears, SGN densities for the entire cochlea were compared between ears in the same mouse and across mice to see group trends (Figure 5).

For comparing histology across species, SGN density and IHC survival for both mice and guinea pigs were divided into three categories of cochlear health: high, medium and low. For presentation in graphs, SGN density was coded in red for SGN densities greater than 700 cells/mm^2, in yellow for SGN densities from 400 - 700 cells/mm^2, and in black for SGN densities less than 400 cells/mm^2. IHC survival was coded similarly with red representing high, yellow medium to low, and black no IHC survival.

2.6 Electrically-Evoked Compound Action Potential Amplitude-Growth Functions (ECAP AGFs)

ECAPs (Figure 6a; electrical responses to stimuli recorded from the auditory nerve, increasing with stimulus strength) were recorded in awake mice while the animals were in their home cage. Recordings were first made 8 or 9 DPI and then every 2 to 7 days until the animal’s end date. Measurements were made twice per session to ensure repeatability of responses. Monopolar electrode configurations were used for stimulation and recording. All electrode stimulating and recording combinations were tested. The primary combination of interest was to stimulate the most apical electrode in the cochlear implant (electrode 1) and record from the adjacent, more basal electrode. The stimulating and recording ground was the ball placed in the muscle just above the bulla. The stimulus level was measured in current units (cu) where 1 cu was approximately equivalent to 1 micro amp (μA). Stimulation and recording utilized a MED-EL “Pulsar” CI100 receiver/stimulator (Innsbruck, Austria) hardwired to a cable that interfaced with the Cochlear® electrode array and the ground ball through the percutaneous electrical connector mounted on the mouse’s skull (Figure 1). The receiver/stimulator was connected to a standard PC through a Research Interface Box (RIB II; University of Innsbruck, Austria). Custom software controlled all measurement parameters.

The ECAP stimulus was a 45 μs phase duration biphasic pulse with a 2.1 μs inter-phase interval. Pulses were delivered at 50 pulses per second (pps) for 20 repetitions. Following electrical pulse onset, the recording amplifier was blanked for 165 μs to avoid saturation artefacts. Prior to recording, the maximum stimulus level (MSL) for each stimulation site was determined. The MSL was based on behavior but was difficult to determine as the mice did not display the standard facial twitch or pinna movement that was useful for determining the upper limit of stimulation in guinea pigs (Pfingst et al., 2017). MSLs were set by gradually increasing the level from 0 cu to the level at which the mouse would seem irritated and excessively ambulate; a clear ECAP response on the ECAP monitor was also required. Once this level was reached the MSL was set 10 cu below this level. To obtain an ECAP AGF, the program selected stimulus levels at 15 amplitudes evenly spaced from zero to the MSL, and presented them in a set order (8, 1, 9, 2, 10, 15, 5, 6, 14, 13, 12, 7, 3, 4, 11).

For every stimulus level, responses to an anodic leading biphasic pulse and a cathodic leading biphasic pulse were averaged to reduce stimulus artifacts. The response to a zero-level stimulus was also recorded and subtracted from this average to reduce non-stimulus related effects like switch-on artifacts. The resulting waveforms (Figure 6a) obtained for each of the 15 levels were plotted and analyzed using a custom-made Matlab program. Negative (N) and positive (P) peaks on the waveform were picked by the program, but were also verified by visual inspection. The N1 to P2 response amplitude was used in μV and was plotted against stimulus current in μA to obtain input-output AGFs. As was previously done in guinea pig (Pfingst et al., 2017), slopes of the AGFs were calculated using only ECAP amplitude response values above 100 μV. A linear regression was applied to fit all data points from this 100 μV to the MSL, providing the ECAP amplitudes continued to increase as a function of level. Means of the AGF slopes obtained on or closest to the day of animal euthanasia were used for comparison to the histological data.

2.7 Electrically-Evoked Auditory Brainstem Response Amplitude-Growth Functions (EABR AGFs)

EABRs (Figure 6b; electrical responses to stimuli recorded from the brainstem, increasing with stimulus strength) were recorded under ketamine (120 mg/kg) and xylazine (7 mg/kg) anesthesia on 8 or 9 DPI, then weekly until the animal's end date. Initially anesthesia was induced with ketamine/xylazine alone, but to reduce the stress of this capture and injection process in later tests, anesthesia was induced with isoflurane followed five minutes later with the ketamine/xylazine injection. A monopolar electrode configuration (electrode 1 to the ground ball) was used for stimulation. EABR responses were recorded from needles placed through the skin. The active needle was on the vertex, the return needle was under the implanted ear, and the ground needle was under the contralateral ear. Neural activity was amplified with a bioamplifier (P55 A.C. Pre-Amplifier; Grass Instrument Co., West Warwick, RI), converted to a digital signal using a TDT AD1, and recorded using the BioSig32 program (Tucker Davis Technologies, Alachua, FL). The bioamplifier was set to a gain of 10,000 and a bandwidth from 0.1 – 3 kHz.

The EABR stimulus was a 25 μs duration monophasic alternating polarity pulse at 50 pps, 2048 pulses per trial. To obtain an input-output AGF, the beginning amplitude was set to a level thought to be below the animal's comfort level. Initially 300 μA was used as this was the safe upper limit determined for our guinea pigs. However, after testing several mice (not included in this study) and seeing balance and mobility issues after anesthesia recovery, the beginning stimulation level was reduced to 225 μA. At this lower current level, there were still occurrences of issues in the second and third mouse implanted, so starting levels were decreased until a level of 150 μA was determined safe for most mice. The last two implanted mice were tested at this current level the first time tested (8 DPI), but after that first day of testing, future starting levels were based on ECAP comfort levels so that comfort levels were not exceeded during the anesthetized EABR test. Stimulus levels were decreased in 5 - 25 μA step intervals until neural responses were too small to be detected reliably. A 0 μA level was also tested to determine the resting noise level and help discriminate small evoked responses from noise. Negative and positive peaks from each waveform (Figure 6b) were manually picked and the N1 to P2 amplitude calculated. The N1 to P2 amplitudes in μV

were plotted against stimulus current in μA to obtain input-output AGFs. To fit the data and to account for measurement error at low stimulus levels, only EABR amplitude response values above 0.25 μV were used to calculate slopes of the AGFs. A linear regression was applied to fit all data points from 0.25 μV to the MSL, provided the EABR amplitudes continued to increase as a function of level. Points that were declining as they approached the MSL, were excluded from the fit. Means of the AGF slopes obtained on or closest to the day of animal euthanasia were used for comparison to the histological data.

2.8 Ensemble Spontaneous Activity (ESA)

ESA recordings (Dolan et al., 1990; Searchfield et al., 2004) were used to measure the amount of spontaneous activity in the auditory nerve and detect the presence of IHCs following implantation. Spontaneous electrical activity was recorded from the cochlear implant electrodes while the animal was under ketamine (120 mg/kg) and xylazine (7 mg/kg) anesthesia, on a heating blanket in a sound-attenuating chamber (Acoustic Systems model AS02893, Austin, TX). To reduce ambient noise contamination in the recording, animals were grounded to the table on which they were resting with a needle placed subcutaneously through the animal's side and a cable from it clipped to the table. ESA levels were tested at 8 or 9 DPI, then weekly until the animal's end date. Electrical potentials were recorded from each electrode in the cochlear implant electrode array using a monopolar recording configuration with the ground being a needle placed under the pinna on the implant side. The recorded electrical potentials were filtered from 300 Hz to 3.0 kHz, amplified with a gain of 10,000, and transmitted to a SR760 spectrum analyzer (Stanford Research Systems, Sunnyvale, CA) which had a sampling rate of 256 kHz. The frequency span of the SR760 was set from zero to 12.5 kHz, which resulted in an analysis window of 32 ms. Using Blackman–Harris windowing, a Fast Fourier Transform (FFT) was performed on each recorded potential. The frequency resolution of the resulting FFT was 31.25 Hz. One hundred fifty records were acquired, transformed and averaged (linear, RMS averaging). The resulting waveforms were retrieved and stored by a Matlab program written in-house. Waveform response levels (dB re 100 μV) from 593.75 Hz to 1312.5 Hz were averaged. Previous studies of guinea pigs with surviving IHCs found a peak in the spectrum in this frequency range if spontaneous neural activity was present. Averages across this range were used instead of peak levels to be able to compare animals with poor health that may not have a distinct peak to those that had better cochlea health and a distinct peak. This range has been represented on the ESA figures by two black vertical lines; at 593.75 Hz and 1312.5 Hz. ESA levels obtained on or closest to the day of animal euthanasia were used for comparison to the histological data.

2.9 Electrode Impedance

Impedances were measured on the day of surgery and then before and/or after ECAP and EABR recordings on 8 or 9 DPI and then every 2 to 7 days until the animal's end date. Monopolar electrode configurations were tested for all electrodes. The stimulus was a 1 kHz sinusoid at 1 μA rms. Impedances obtained on or closest to the day of animal euthanasia were used for comparison to the histological data.

2.10 Guinea Pig Comparison Data

Mouse data were compared to data from long-term stable chronically-implanted guinea pigs to help interpret results and establish the mouse as a comparable candidate for cochlear implant studies. The comparison was made to a subset of the multichannel implanted guinea data previously published (Pfingst et al., 2017). Data presented here include ECAP and EABR AGFs, ESA, impedance, and histology collected from guinea pigs with good cochlear health (implanted–hearing; N = 23) and poor cochlear health (neomycin deafened-implanted or neomycin deafened AAV.Empty-implanted; N = 14). Guinea pigs from these two groups were used because they have a wide range of cochlear health to compare to the implanted mice. Survival times ranged between 131 – 640 DPI. Impedance data were collected for all 37 guinea pigs, but one guinea pig had an implant failure so impedances are presented for only 36 guinea pigs. For the rest of the measures, data were collected from only a subset of these guinea pigs. Below are simplified descriptions of procedures performed on the guinea pigs. Detailed descriptions of all these procedures have previously been described (Pfingst et al., 2017).

Surgical procedures were performed under ketamine (40 mg/kg) and xylazine (10 mg/kg) anesthesia. Ears that were deafened were done either via neomycin sulfate (10 μl; 5 % w/v) slowly injected into the scala tympani through a cochleostomy using a cannula and an infusion pump at a rate of 5 μl/ minute (N = 6), or (60 μl, 10 % w/v) slowly injected through the round window with a needle and syringe (N = 8). For both implanted-hearing and neomycin deafened-implanted ears, implants were inserted into the scala tympani via a cochleostomy drilled in the basal turn of the cochlea.

Implants for the guinea pigs consisted of 8 ring electrodes encircling a silicone rubber carrier and spaced at 0.75 mm center to center (Cochlear® 8 ring animal array). The diameter of the implant near its apical end was 0.4 mm so that it filled the majority of the scala tympani at about 4.5 mm from the cochleostomy. The primary electrode used for stimulation (ECAP and EABR) in the guinea pigs was the second most apical electrode, which was located an average of 2.7 mm apical to the cochleostomy (approximately the 18 kHz region) and typically sat close to the modiolar wall, and was ground to a small inverted bolt anchored to the skull with three screws. Recording electrodes and return grounds were tested in the following combinations for the various measurements: an electrode adjacent to the primary electrode ground to a recording screw on the skull (ECAP), two screws on the skull (EABR), all electrodes individually to the bolt on the skull (ESA), and all electrodes individually to the ball electrode in the neck (impedances).

Histological data for the guinea pigs (mid-modiolar sections, SGN densities and IHC assessments) were obtained in a fashion similar to that described for the mice. Histological data for 10 non-implanted “normal” guinea pig ears were used for comparison to implanted guinea pigs. Intrascalar tissue and new bone references were taken from Swiderski et al., 2020 where a thorough analysis of these tissues was performed. Thirty-three of the guinea pigs presented in the current study were included in our recent publication (Swiderski et al., 2020).

ECAP, EABR, and ESA recordings as well as impedances were performed using the same equipment and procedures described above for the mice except for the following differences: for the guinea pigs ECAP MSLs were determined by an observed facial twitch or pinna movement and set about 10 cu below the current level eliciting one of these facial nerve responses, ECAP and EABR starting stimulation levels were higher, anesthesia doses were higher, and the return grounds were as specified in the guinea pig implant paragraph above.

3. Results

3.1 SGN and IHC Survival and Intrascalar Tissue Density

Histological examination of the five implanted mouse ears revealed that SGN densities in the area of the implant were 342 - 1227 cells/mm^2 (Table 1 Profile A, Figure 5). The range of SGN densities for these five implanted ears was quite broad with the lowest SGN densities coming from the implanted ears of mouse 7628 and 7708. SGNs in these ears showed signs of being unhealthy (enlarged). For the five non-implanted normal contralateral comparison mouse ears, SGN densities were 506 – 1629 cells/mm^2 for the same profile. The range of SGN densities for these five non-implanted ears was also quite broad with the lowest SGN densities coming from the contralateral ears of the same two mice as above (7628 and 7708). These mice prior to implantation had normal hearing in their left ears (confirmed by ABR), but at the time of histology had lower SGN density in Profile A of both their left and right ears. In their non-implanted ears, both mice had unhealthy (shrunken) SGNs and other anomalies. When comparing SGN densities for Profile A (the area of the implant) within mice, four implanted ears had SGN densities that fell in the range of their contralateral ears and one implanted ear (7592L1) had lower SGN density than its contralateral ear (Figure 5). Statistical analyses between the two ears was not performed as the ranges of variation in both groups were so broad that we could not say with confidence what the expected values were for either group.

Apical to the implant, SGN densities were 454 – 1761 cells/ mm^2 (Table 1 Profiles B and C; Figure 5) for the implanted ears. For these same profiles in the non-implanted ears, SGN densities were 566 – 2068 cells/ mm^2. All implanted ears were in the range of their contralateral non-implanted ears for either one or both profiles B and C. In mouse 7592 Profile B had lower SGN density than its non-implanted ear, and for mouse 7627, 7628 and 7707 Profile C (in the apex) had lower SGN density than their non-implanted ears showing that variable damage can occur apical to the implant.

IHC survival in the area of the implant (Table 1 Profile A) varied across mice with some ears having normal IHC survival (Table 1 “high”; Figure 4b), missing IHCs (Table 1 “medium or low”), and no IHCs with either supporting cells (Table 1 “absent”; Figure 4a), or a flat epithelial layer (Table 1 “absent”; Figure 4c). Apical to the implant, all mice had surviving IHCs (Table 1 Profiles B and C), but mouse 7628L1 had a decreasing gradient (high, low, 0) of surviving cells from base to apex. In four non-implanted contralateral ears, IHC survival for Profiles A through C was normal (high); a representative example of this survival in the organ of Corti can be seen in Figure 4d. However, for the non-implanted ear of mouse 7708, IHC survival for Profile A was medium and Profile B absent; Profile C was not assessable due to histology complications.

Intrascalar tissue was observed in Profile A (e.g., Figure 2) of all implanted mice, with two mice having some in Profile B as well. Intrascalar tissue was of high density in Profile A for four mice and of low density for one mouse (7627L1). New bone was seen for two mice in Profile A (7628L1 and 7708L1) and two mice in Profile B (7592L1 and 7628L1).

Histology performed on the 37 implanted guinea pig ears revealed SGN densities in the area of the implant (Profile A) ranged from 307 - 1221 cells/mm^2 for the implanted-hearing guinea pigs and from 6 - 211 cells/mm^2 for the neomycin deafened-implanted guinea pigs. For the ten non-implanted normal guinea pig comparison ears, SGN densities for Profile A ranged from 727 to 1287 cells/mm^2. Only five of the 23 implanted-hearing ears had SGN densities in Profile A lower than the range for the normal non-implanted ears. For profiles apical to the implant (Profiles B and C) SGN densities ranged from 561 - 1293 cells/mm^2 for the implanted-hearing guinea pig ears, 6 - 211 cells/mm^2 for the neomycin deafened-implanted guinea pig ears and 767 - 1519 cells/mm^2 for the non-implanted normal guinea pig comparison ears. IHC survival across Profiles A through C ranged from high to 0 with the majority (N = 18) of the implanted-hearing guinea pig ears having high IHC survival for all Profiles from A through C and the remaining five having 0 IHC survival in at least one profile but medium to high survival in the other two profiles. For the non-implanted guinea pig ears, IHC survival for Profiles A through C was normal (high). For the neomycin deafened-implanted guinea pig ears, IHC survival across Profiles A through C was 0. Intrascalar tissue and neo-ostenogenesis was present with the lowest occurrence of both in implanted-hearing ears and the highest occurrence in ears treated with neomycin (Swiderski et al., 2020). The degree and variation in formation seem to be dependent on the local trauma associated with implant insertion and ear manipulation (i.e. infusion of neomycin, etc.).

When comparing across species, the implanted mice and guinea pigs had comparable amounts of SGN and IHC survival throughout the cochlea. Where they differed was in the amount of intrascalar tissue present in the area of the implant. The implanted-hearing guinea pig ears had the lowest occurrence of both intrascalar tissue and neo-osteogenesis while four out of five mouse ears had high density intrascalar tissue in the area the implant and two of these also had new bone formation.

3.2 ECAP AGFs and Slopes Over Time

For four mice, ECAP data were collected up to 42 DPI. ECAP AGFs (neural response magnitude versus stimulus current level) for two mice with multiple measurements over time (7707L1 and 7708L1) showed changes in sensitivity after implantation similar to those seen in guinea pigs with slopes either improving to a steady state or stabilizing at lower levels. AGF slopes for mouse 7707L1 improved to a steady state (slopes reached a plateau) for all three of its electrodes (Figure 7a1 - 3 and guinea pig comparison c). AGF slopes for mouse 7708L1 stabilized at lower levels for both of its electrodes (Figure 7b1 - 2, and guinea pig comparison d). Slopes over time for these two mice for all measurable electrodes showed patterns similar to guinea pigs with comparable cochlear health, but AGF slopes for mice appeared to plateau more quickly at approximately 15 and 8 DPI. Slopes for guinea pigs with similar SGN densities typically take much longer to recover with plateauing beginning

around 13 to 120 DPI as shown for a few samples here (Figure 7c and d) and presented in previous publications (Su et al., 2008, and Pfingst et al., 2015).

ECAP AGFs and slopes were plotted as a function of SGN density in Profiles A through C (Figure 8). The two mice in which we were able to collect data over a longer period of time (42 DPI) and that were at a plateau, were plotted for comparison to the long-term stable guinea pigs. In general, these two mice had similar AGFs to the guinea pigs and as shown in Pfingst et al., 2017, animals with higher SGN densities tended to have steeper slopes of the ECAP growth functions. The mouse represented by the star (7707L1, Figure 8a) showed a steeper growth in responses as current was increased and also had a steeper slope than all of the guinea pigs presented here (Figure 8b and c). However, guinea pigs with good cochlear health can have AGF slopes that range from approximately 6 – 22 μV/μA (data not shown). Our data show that in mice, as in guinea pigs, animals with good cochlear health (IHCs present and high SGN density) can have a broad range of ECAP AGF slopes, but those slopes are still steeper than animals with low SGN density and no IHCs (Figure 8c).

One notable difference between these two mice and the guinea pigs was in the amount of current needed to evoke an ECAP response. Levels and comfort ranges for the mice were much lower/smaller than those for the guinea pigs (Figure 8a and b). Growth of ECAP AGFs for the mice began at approximately 50 to 100 μA (2.25 to 4.5 nanocoulomb (nC)) with upper limits for stimulation ranging approximately from 100 to 200 μA (4.5 to 9.0 nC). This threshold and comfort range was consistent with data reported for neural response telemetry (Claussen et al., 2019). Growth of ECAP AGFs for the guinea pigs began at approximately 100 to 150 μA (4.5 to 6.75 nC) with upper limits for stimulation ranging approximately from 200 to 300 μA (9.0 to 13.5 nC).

3.3 EABR AGFs and Slopes Over Time

For four mice, EABR data were collected up to 42 DPI. EABR AGFs and slopes for the two mice with multiple measurements overtime (7707L1 and 7708L1) and guinea pigs (Figure 9) showed some changes in sensitivity over time after implantation, but patterns were not as consistent or obvious as compared to the ECAP data. The pattern of recovery for these two mice were similar to guinea pigs: EABR AGFs for mouse 7707L1, who had better cochlear health in the area of the implant, showed changes over time similar to guinea pigs with better cochlear health (Figure 9a and c), and mouse 7708L1, who had poorer cochlear health in the area of the implant, showed no recovery and stabilized at lower levels similar to guinea pigs with poorer cochlear health (Figure 9b and d). Within animals, patterns of recovery and change were not the same across the implant as seen for mouse 7707L1 electrode 1 and 2 (Figure 9a1 and 2). Slopes over time for both electrodes showed an increase in sensitivity followed by a decrease in sensitivity on 19 DPI, but slopes for electrode 1 appear to be stabilizing while slopes for electrode 2 were still increasing on 42 DPI. A completely different pattern was seen for mouse 7708L1 (Figure 9b); slopes over time showed a more gradual increase in sensitivity over a course of 10 days followed by a decrease in sensitivity up to 42 DPI. Without long-term data on more mice, it was difficult to determine if these were normal fluctuations in data or real trends. Slopes overtime for guinea pigs showed

some fluctuations, but most slopes were stable as early as 30 to 90 DPI; without earlier data in the guinea pigs, changes comparable to the mice were not discernable.

EABR AGFs and slopes were plotted as a function of SGN density in Profiles A through C (Figure 10) for four mice and multiple long-term stable guinea pigs of various cochlear health. In general, the mice had similar AGFs to the guinea pigs with comparable cochlear health (red and yellow lines), and as shown in Pfingst et al., 2017, animals with higher SGN densities tended to have steeper slopes of the EABR AGFs. Mouse 7707L1 (Figure 10a; red star) showed a steeper growth in responses as current was increased, compared to the other three mice and the guinea pigs. When comparing slopes of the mice AGFs to those of the guinea pigs (Figure 10c), the other three mice were in a similar range to the guinea pigs with comparable cochlear health, and mouse 7707L1 falls in a reasonable range to the rest of the animals.

As with the ECAP AGFs, for the EABR AGFs there was also a notable difference between the mice and guinea pigs in the amount of current needed to evoke an EABR response. Levels and comfort ranges for the mice were much lower/smaller than those for the guinea pigs (Figure 10a and b). Growth of ECAP AGFs for the mice began at approximately 25 to 100 μA (0.625 to 2.5 nC) with upper limits for stimulation ranging approximately from 100 to 225 μA (2.5 to 5.625 nC). This threshold and comfort range was lower than those reported for EABR (Irving et al., 2013; Navntoft et al., 2019). Growth of ECAP AGFs for the guinea pigs began at approximately 125 to 300 μA (3.125 to 7.5 nC) with upper limits for stimulation ranging approximately from 350 to 500 μA (8.75 to 12.5 nC). Results for EABR AGFs and slopes were more difficult to compare across species due to measurement ranges starting early in the mice (8 DPI) and being measured weekly but ending before or by 42 DPI, and later in the guinea pigs starting 28 - 31 DPI and being measured approximately every 30 days until euthanasia.

3.4 ESA

ESA data were collected up to 42 DPI for four mice. ESA levels for the two mice with multiple measurements overtime (7707L1 and 7708L1) showed changes in spontaneous activity after implantation with ESA levels still showing signs of recovery by 42 DPI which was the last day tested (Figure 11a and b). This long recovery time was not unusual, as guinea pigs with varying cochlear health also showed spontaneous activity increases up to 92 DPI (Figure 11c and d); even guinea pigs that were deafened and had no remaining IHCs showed this pattern (Figure 11d). Since we were unable to collect data beyond 42 DPI in the mice, we could not determine if the spontaneous activity in mice recovered quicker or within the same time course as the guinea pigs; ESA levels for both mice were still increasing at 42 DPI (Figure 11a and b).

One difference between the mice and guinea pigs was in the presence of the clear peak in the ESA spectra near 900 Hz which has been seen in guinea pigs with high numbers of surviving IHCs (Figure 11c and 12b, red and yellow lines). This peak was present in the mice but was much less defined and the spectra noisier (Figure 11a and 12a) as repeating noise can be seen in all the mice spectra. Further testing will need to be done to determine the source of the noise and if the peak would become more pronounced with it removed.

ESA averaged levels (levels averaged over the frequency range in which a “normal” peak response was seen in guinea pigs; frequencies from 593.75 Hz to 1312.5 Hz) were plotted as a function of SGN density in Profiles A through C (Figure 12c). Final averaged ESA levels for three of the mice were in a range similar to those reported for long-term cochlear-implanted guinea pigs with comparable cochlear health, but mouse 7628L1 had a lower averaged ESA level and a lower SGN density than all other mice and guinea pigs with better cochlear health (red and yellow circles).

3.5 Impedance

Impedance data over time were collected up to 42 DPI for all five mice. Impedances for the first three implanted mice showed electrode failures within the first 16 days. The remaining two mice (Figure 13a and b) were measured up to 42 DPI. Impedances in mice and guinea pigs were similar in changes over time with impedances for individual electrodes showing one of four trends: 1) impedances that have a gradual increase and then stabilize (Figure 13a mouse electrode 1-G; 13c guinea pig electrodes 4, 5 and 6-G); 2) impedances that have a gradual increase and then decrease to a steady state (Figure 13a mouse electrodes 2 and 3-G; 13c guinea pig electrode 3-G and 13d guinea pig electrodes 1, 4, 5 and 6-G); 3) impedances that have a decrease to a steady state (Figure 13b mouse electrode 3-G; also present in guinea pigs but not seen in these two examples); and 4) impedances that show no change (Figure 13b mouse electrodes 1 and 2-G; 13c guinea pig electrodes 1 and 2-G, and 13d guinea pig electrodes 2 and 3-G). The time course of impedance change seems to be similar for mice and guinea pigs as changes begin within days of implantation for both groups (Figure 13) and then stabilize within similar ranges of DPI (anywhere from 8 to 26 DPI).

One notable difference between the mice and guinea pigs was in the absolute stable impedance. Impedances for the mouse electrodes were in the range of 10 to 30 kOhms (except for electrodes that were broken) and impedances for guinea pig electrodes were in the range of 4 to 22 kOhms (Figure 13).

3.6 Complications

Functional data collection ended earlier than planned due to one or more of several complications: implant failure, spontaneous death following anesthetic administration and/or overstimulation (before or after EABR and ESA recordings), or percutaneous connector instability.

Implant failure occurred quickly in the first three implanted mice with suture-secured implants; within 8 to 23 DPI all three electrodes on all three implants had broken. Since implants in these three mice failed quickly, implants in the last two mice were not sutured but left free under the skin to move as the mouse moved; implants were only secured with Durelon at the bulla. In these last two mice, implant breakage was not the cause of termination. These non-suture-secured implants were our two longest surviving implants at 42 and 46 DPI. On these two implants, all electrodes were functional for the entire life of the mouse.

Three out of five mice died from complications of anesthesia and/or overstimulation: one immediately after anesthesia induction, and two after completion of all tests for the day. The

mouse that died after anesthesia induction was one of the first mice implanted and tested. To prevent anesthesia-related deaths in future mice, we began using the two-stage anesthesia method described in the EABR methods section. Following implementation of this method, no additional mice died after anesthesia injection. However, there were complications of two mice dying after completion of tests and while coming out of anesthesia. These mice showed signs of manic behavior and inability to maintain a sternal position. To reduce mice dying following testing, we lowered starting stimulation current levels for EABR and ECAP recordings, and based upper limits for both on observed behaviors while raising levels during a real-time test for ECAP response. Further testing will be needed to establish if either multiple doses of anesthesia and/or overstimulation could have caused complications with the recovery of the mice post-procedure.

One out of five mice had their percutaneous connector come off when plugging in the cable for ECAP testing on 46 DPI; for this mouse (7707L1), measurements for all tests were last taken on 42 DPI. Prior to implementing the method for attaching the implant base described in this manuscript, several other methods of base attachment were tested including combinations of the following: skulls scraped and scored for greater adhesion, use of super glue between the skull and acrylic, one screw and dental acrylic, multiple screws, removal of skin around the acrylic and attachment of acrylic to the skin edges. Most of these methods were not stable enough for daily pushing and pulling to connect and disconnect cables used for testing or for the general activity of the mice (feeding, grooming, and hitting their heads on plastic housing cages); also in some cases, skin surrounding the connector grew under the edges and pushed the acrylic off the skull. The method that worked best for us for most animals was cleaning the skull with hydrogen peroxide, applying acrylic to multiple screws distributed around the skull, and trimming skin edges around the acrylic.

4. Discussion

In this study, we have shown that long-term (up to 42 DPI) daily electrophysiological recordings in cochlear-implanted mice are feasible, thereby extending the duration of implantation and testing relative to previous studies (Irving et al., 2013; Soken et al., 2013, Mistry et al., 2014; Navntoft et al., 2019; Claussen et al., 2019). We also pioneered the use of ESA recording in cochlear-implanted mice. We determined that ECAP in awake mice is a safer measure of implant function and cochlear health in mice, compared to the EABR recording under anesthesia. We found that cochlear implant outcomes in the mouse model were similar to those obtained in guinea pigs in some, but not all, aspects.

Histologically the mice were very similar to the guinea pigs, in that ears with better cochlear health in the area of the implant had better responses. In comparing implanted and non-implanted ears within mice, we were able to see pre-existing ear conditions in several mice and more effectively assess the degree of trauma induced in the implanted ears. The damage and additional damage seen in some implanted ears, we believe, was potentially a result of multiple factors induced at the time of implantation including damage caused by implant insertion trauma (i.e. physical trauma to walls and membranes, displacement and motion force in the perilymph, etc.); blood, bone, tissue, and/or Durelon cement that may have extruded into the scala tympani; and the immune reaction to the implant. Due to the small

size of the mouse cochlea and the bulla, implant insertion and bulla closure with Durelon can be challenging. In addition, the high intra-cochlear perilymph pressure of the mouse cochlea can produce a large flow of perilymph into the bulla area after puncture of the round window membrane, making closure with the cement difficult because perilymph can mix with the cement before it has sufficiently hardened. Placement of a muscle plug on the round window to help reduce perilymph flow and keep the implant from migrating out is an imperfect solution because it likely contributes to cochlear inflammation and a tissue fibrosis response (Burghard et al., 2014). In our study, all mice had various degrees of fibrosis and new bone in the scala tympani. Several other studies on cochlear implants in mice have described fibrosis and bone in the scala tympani (Irving et al., 2013; Mistry et al., 2014; Claussen et al., 2019). These studies used various surgical methods which all resulted in fibrosis and bone growth. Further work is needed to identify which of the experimental manipulations is the primary or dominant cause of these tissue reactions, i.e., drilling, insertion, presence of foreign body, or stimulation.

Previous studies have shown that electrophysiology measurements such as ECAPs and EABRs are highly correlated with SGN density and are easily measured in many implanted species (Smith and Simmons, 1983; Hall, 1990; Pfingst et al., 2015). Results here suggest that this is the case for mice as well, as results for mice were similar to implanted guinea pigs in both patterns over time after implant insertion and AGF slope. One area of difference was that stimulation levels and ranges to evoke responses were lower in mice; this was not surprising given the differences in head size between these species. For instance, in the mouse, implants may sit closer to the stimulating tissues, bone thickness differs, and electrical currents may travel in different paths, which could account for some of the differences between species. Also at comparable current levels, current could travel relatively further in the much smaller sized mouse. High current levels that reach only cochlear elements in the guinea pig might stimulate areas beyond the cochlea such as the vestibular system and the brain in the mouse. We may have seen evidence of this in that two mice showed signs of manic behavior and inability to maintain a sternal position following testing of EABR, ESA and ECAP on the same day. Because multiple tests were run that involved measuring upper limits of stimulation (EABR and ECAP), the behavior might have been a result of current levels being too high for one or both tests. However, we cannot rule out that the behavior may have been a complication from multiple anesthetic doses given for testing both EABR and ESA on the same day.

Determining safe upper limits in the mice was difficult. In our studies with guinea pigs, we used facial nerve stimulation (pinna twitch, whisker twitch, eye twitch, neck twitch) to determine safe and comfortable stimulation levels, but mice did not display these characteristics at higher current levels. When mice were anesthetized for EABR testing, safe current levels could only be based on muscle artifact evoked at higher levels on the EABR waveform (but not visually in the animal), which at times may have been too high. In guinea pigs, sensitivity to electrical stimulation changes rapidly in the first 30 DPI and can still be changing up to 120 DPI (Su et al., 2008; Pfingst et al., 2015). We showed evidence that this is the case for mice as well; a comfortable or safe level one day might be uncomfortable or unsafe on another day until stability has been reached. Therefore, another advantage of the ECAP over the EABR is that animals are awake, and setting safe current levels can be based

on animal behavior, not just muscle artifact evoked at higher current levels as with EABR. Also, because mice can be susceptible to stress from manipulation and repeated anesthetic injections, procedures that involve anesthesia can become life threatening and detrimental to completion of long-term studies. Given these risk factors and the similarity in results with these two measures, the ECAP is a safer choice for chronic long-term electrophysiological studies in mice.

ESA can be a useful test for periodic assessment of the spontaneous activity in the auditory nerve and the presence of functioning hair cells (Dolan et al., 1990; Searchfield et al., 2004). ESA was recorded under anesthesia, but the small size of the mouse and its ability to metabolize anesthesia more rapidly than the guinea pig meant that the depth of anesthesia when ESA was recorded after EABR was light. This could be the reason for the noisier ESA recordings in mice compared to those in guinea pigs. Nevertheless, mice were comparable to the guinea pigs in ESA average level and recovery trends. Because our data set was small and responses might not have reached stable activity levels during the period over which the mice were tested, the time course for recovery of this measure in mice was unclear. For the two mice that were testable up to 42 DPI, spontaneous activity was continuing to increase over time, so additional mice will need to be tested to determine what normal long-term stable responses look like for mice. In this study, we also averaged the ESA levels over the frequency range in which a response peak is normally seen in guinea pigs with residual IHCs. Given that mice seem to require less current to evoke ECAPs and their acoustic hearing range differs from guinea pigs, it is possible that the peak of the ESA for mice does not fall in the same range as that of guinea pigs. Results to date suggest that these two species can be compared in this method, but increased numbers of mice with varying degrees of cochlear health will help define if the response peaks around 900 Hz or elsewhere for mice.

Impedances in mice, as in guinea pigs, showed a large variety of changes over time both between animals and within a given animal. Other studies have described similar results and suggested that patterns of slower, gradual increases in impedance over time could represent evidence of accumulation of fibrous tissue and new bone formation around the implant as part of an inflammatory response (Irving et al., 2013; Claussen et al., 2019). In our study, this could be the case for some stimulation sites that have a gradual increase and then stabilize, but it does not support the other three trends we saw in both mice and guinea pigs: 1) impedances that show a gradual increase and then decrease to a steady state; 2) impedances that have a decrease to a steady state; and 3) impedances that show no change. These trends suggest that multiple factors affect impedance and are more complex than we can explain in this study.

Impedance is a useful tool for determining implant integrity. When impedance increased drastically, it was most likely a sign of implant instability and breakage, as seen in the first 3 implanted mice in this study and also reported previously (Claussen et al., 2019). One difference in impedance between mice and guinea pigs was in the stable impedance level, which was larger in mice than in guinea pigs. This was most likely due to the smaller size of the scala tympani space in the mouse cochlea and the smaller surface area of the mouse electrodes.

Multiple complications (implant failure, spontaneous animal death, or percutaneous connector instability) caused data collection to end earlier than planned, which undoubtedly impacted our ability to accomplish the goal of collecting long-term stable data in a larger cohort of mice. Progress toward this goal was achieved in the last two implanted mice, as data for most of the measures (except for ESA level) reached what appeared to be a steady state. Unfortunately, we have not yet obtained data beyond 42 DPI, which is still within the range of when measures change for many implanted guinea pigs. We need to increase our numbers of long-term implanted mice to fully understand trends for hearing-implanted mice and eventually mice with a variety of hearing deficiencies. Reasons for some of these complications and ways of improving outcomes are discussed below.

Implant failure was the first issue that we addressed after early implant failures in the first three mice. Mice are very active and spend much more time grooming than guinea pigs and because we had not tested these first three mice often before their implants failed, we concluded that the implants may have been failing as a complication of suturing the implants to the muscle rather than from handling we did to be able to plug in and test the implants. Since these wires were fixed and not allowed to move freely, they may have broken due to wire fatigue from excessive head and neck motion. Electrode longevity improved when implants were instead left free under the skin to move as the mouse moved; this might account for the much longer implant survival times seen in the last two implanted mice. However, we cannot rule out that increased longevity in these last two mice were a result of surgical practice in handling and inserting these multichannel implants. Over 25 implant surgeries in mice had been performed by this same surgeon prior to these multichannel implant surgeries except with a single channel implant made in-house that had different mechanical properties from these commercially made implants. Despite having significant experience implanting mice, the device property differences could have increased the probability of implant damage during the first few multichannel implant surgeries until the surgeon became familiar with how this implant handled relative to the implants made in-house.

Another complication was mice spontaneously dying before and after procedures. To reduce the occurrence of spontaneous death, we modified both our anesthesia induction process and our EABR starting and maximum current stimulation levels. We also used a non-anesthesia test, the ECAP, to reduce stress. ECAPs can be performed while mice are in their home cages with minimal handling. ECAPs are also effective measures of cochlear health in most cases, even when animals have poor cochlear health. We have seen in some implanted guinea pigs with poor cochlear health that ECAPs were not measureable due to tolerable comfort levels being reached before ECAP responses could be evoked, but for the majority of animals, measurable responses were possible. If tests under anesthesia are necessary in future studies, we will test less often (i.e. on 0 DPI and the last day for functional testing with maybe a point or two in between) and use a two-stage anesthesia method. After implementing isoflurane induction before injecting anesthetic, we had no further immediate post-anesthesia deaths which we believed were due to stress-induced tachycardia resulting in myocardial infarction that can be caused when using a capture and inject anesthesia technique. Also, increased animal handling prior to surgery and functional measurements can also lead to better outcomes.

To reduce possible overstimulation and damage to the mice, we reduced upper stimulation levels to less than 250 μA (i.e. less than 11.25 nC for ECAP and less than 6.25 nC for EABR) and used upper limits for EABR and ECAP recordings based on observed behaviors of mice when recording ECAP in the awake state. During ECAP tests if mice became irritable or more active, the stimulus level at which that occurred was set as the upper limit for that mouse for future tests for both ECAPs and EABRs. Further testing will help establish if either multiple doses of anesthesia and/or overstimulation could have caused complications with the recovery of the mice post-procedure, although we did see a worsening of symptoms over time for several pilot mice (not included in this study) following multiple weeks of testing which weighs more heavily to the overstimulation theory.

One final complication we encountered was detachment of the percutaneous connector when plugging in the cable for ECAP testing. We tested multiple materials and adhesion compounds to secure the percutaneous connector to the skull for our long-term studies, but were not able to maintain stability consistently enough for the longevity of these experiments. In future experiments, possible solutions to explore would be other types of bone cement that adhere more strongly to the surface of the skull, to modify connectors and cables used for testing to prevent less strain on the percutaneous connector, or to use a wireless implant. Irving et al., 2013 used a fully implantable stimulator driven by an external magnetic coil assembly to stimulate implanted mice and to record magnetically-induced electrically-evoked auditory brainstem responses (mEABR). Mice were awake during the chronic stimulation but were anesthetized for the mEABR recordings once again posing an additional risk for anesthetic death and limiting the ability to record data daily in a long-term study. To date, other limitations of these fully implantable devices are that they are not currently commercially available, and that in order to keep them smaller in size stimulus parameters are usually very limited, which reduces their utility for ECAP and psychophysical testing that require more complex stimuli and stimulators.

5. Conclusions

In this study we have shown how implant insertion trauma and stimulation over time post implantation can affect the anatomy and the function of the implanted mouse ear. The data stress the importance of measuring functional responses once the implanted ear has reached a steady state. For long-term studies, we have discussed the difficulties associated with frequent anesthesia required for repeated measures of EABR and ESA, and that ECAP is a safer measure of implant function and cochlear health in mice. Also, the use of ECAPs for long-term frequent testing in the awake state can improve outcomes and allow for effective monitoring of changes over time and stabilization of function post-implantation. Finally, we have shown how a chronic cochlear-implanted mouse is a good model for research on cochlear implant function due to it similarities to an already proven guinea pig model (Pfingst et al., 2017).

While cochlear implant research in mice is possible and important, the technique can be challenging. Improvements in the model are needed to extend the length of the experiments. Once this has been accomplished, further studies can be done to determine the relationship

that long-term stable function and perception have with various cochlear conditions. The mouse model will also be useful for studies of the mechanisms underlying functional changes over time after cochlear implant insertion and lead to improved long-term outcomes for cochlear implant recipients.

Acknowledgements

This work was supported by NIH/NIDCD grants R01-DC015809, R01-DC014832, P30-DC005188, and T32-DC005356.

References

Burghard A, Lenarz T, Kral A, Paasche G 2014. Insertion site and sealing technique affect residual hearing and tissue formation after cochlear implantation. Hear Res 312, 21–7. doi:10.1016/j.heares.2014.02.002. [PubMed: 24566091]

Claussen AD, Vielman Quevedo R, Mostaert B, Kirk JR, Dueck WF, Hansen MR 2019. A mouse model of cochlear implantation with chronic electric stimulation. PLoS One 14, e0215407. doi:10.1371/journal.pone.0215407. [PubMed: 30998726]

DeVries L, Scheperle R, Bierer JA 2016. Assessing the electrode-neuron interface with the electrically evoked compound action potential, electrode position, and behavioral thresholds. J Assoc Res Otolaryngol 17, 237–52. doi:10.1007/s10162-016-0557-9. [PubMed: 26926152]

Dolan DF, Nuttall AL, Avinash G 1990. Asynchronous neural activity recorded from the round window. J Acoust Soc Am 87, 2621–2627. doi: 10.1121/1.399054. [PubMed: 2373796]

Duan YY, Clark GM, Cowan RS 2004, A study of intra-cochlear electrodes and tissue interface by electrochemical impedance methods in vivo. Biomaterials 25:3813–3828. doi: 10.1016/j.biomaterials.2003.09.107. [PubMed: 15020157]

Hall RD 1990. Estimation of surviving spiral ganglion cells in the deaf rat using the electrically evoked auditory brainstem response. Hear Res 49, 155–168. doi: 10.1016/0378-5955(90)90102-u. [PubMed: 2292495]

Irving S, Trotter MI, Fallon JB, Millard RE, Shepherd RK, Wise AK 2013. Cochlear implantation for chronic electrical stimulation in the mouse. Hear Res 306, 37–45. doi:10.1016/j.heares.2013.09.005. [PubMed: 24055621]

Kamakura T, Nadol JB Jr. 2016. Correlation between word recognition score and intracochlear new bone and fibrous tissue after cochlear implantation in the human. Hear Res 339, 132–41. doi:10.1016/j.heares.2016.06.015. [PubMed: 27371868]

Kang SY, Colesa DJ, Swiderski DL, Su GL, Raphael Y, Pfingst BE 2010. Effects of hearing preservation on psychophysical responses to cochlear implant stimulation. J Assoc Res Otolaryngol 11,245–65. doi:10.1007/s10162-009-0194-7. [PubMed: 19902297]

Kim JR, Abbas PJ, Brown CJ, Etler CP, O'Brien S, Kim LS 2010. The relationship between electrically evoked compound action potential and speech perception: A study in cochlear implant users with short electrode array. Otol Neurotol 31, 1041–8. doi:10.1097/MAO.0b013e3181ec1d92. [PubMed: 20634770]

Kurioka T, Lee MY, Heeringa AN, Beyer LA, Swiderski DL, Kanicki AC, Kabara LL, Dolan DF, Shore SE, Raphael Y 2016. Selective hair cell ablation and noise exposure lead to different patterns of changes in the cochlea and the cochlear nucleus. Neuroscience 332, 242–57. doi:10.1016/j.neuroscience.2016.07.001. [PubMed: 27403879]

Mistry N, Nolan LS, Saeed SR, Forge A, Taylor RR 2014. Cochlear implantation in the mouse via the round window: Effects of array insertion. Hear Res 312, 81–90. doi:10.1016/j.heares.2014.03.005. [PubMed: 24657211]

Navntoft CA, Marozeau J, Barkat TR 2019. Cochlear implant surgery and electrically-evoked auditory brainstem response recordings in c57bl/6 mice. J Vis Exp 143, e58073. doi:10.3791/58073.

Newbold C, Mergen S, Richardson R, Seligman P, Millard R, Cowan R, Shepherd R, 2014. Impedance changes in chronically implanted and stimulated cochlear implant electrodes. Cochlear Implants Int 2014 15(4): 191–9. doi:10.1179/1754762813Y.0000000050.

Ohlemiller KK, Jones SM, Johnson KR 2016. Application of mouse models to research in hearing and balance. J Assoc Res Otolaryngol 17, 493–523. doi:10.1007/s10162-016-0589-1. [PubMed: 27752925]

Okayasu T, Quesnel AM, O'Malley JT, Kamakura T, Nadol JB Jr. 2020. The distribution and prevalence of macrophages in the cochlea following cochlear implantation in the human: An immunohistochemical study using anti-iba1 antibody. Otol Neurotol 41, e304–e316. doi: 10.1097/MAO.0000000000002495. [PubMed: 31821256]

Pfingst BE 1990. Changes over time in thresholds for electrical stimulation of the cochlea. Hear Res 50, 225–236. doi: 10.1016/0378-5955(90)90047-s. [PubMed: 2076974]

Pfingst BE, Colesa DJ, Swiderski DL, Hughes AP, Strahl SB, Sinan M, Raphael Y 2017. Neurotrophin gene therapy in deafened ears with cochlear implants: Long-term effects on nerve survival and functional measures. J Assoc Res Otolaryngol 18, 731–750. doi:10.1007/s10162-017-0633-9. [PubMed: 28776202]

Pfingst BE, Zhou N, Colesa DJ, Watts MM, Strahl SB, Garadat SN, Schvartz-Leyzac KC, Budenz CL, Raphael Y, Zwolan TA 2015. Importance of cochlear health for implant function. Hear Res 322, 77–88. doi:10.1016/j.heares.2014.09.009. [PubMed: 25261772]

Prado-Guitierrez P, Fewster LM, Heasman JM, McKay CM, Shepherd RK 2006. Effect of interphase gap and pulse duration on electrically evoked potentials is correlated with auditory nerve survival. Hear Res 215, 47–55. doi:10.1016/j.heares.2006.03.006. [PubMed: 16644157]

Ramekers D, Versnel H, Strahl SB, Smeets EM, Klis SF, Grolman W 2014. Auditory-nerve responses to varied inter-phase gap and phase duration of the electric pulse stimulus as predictors for neuronal degeneration. J Assoc Res Otolaryngol 15, 187–202. doi:10.1007/s10162-013-0440-x. [PubMed: 24469861]

Schvartz-Leyzac KC, Colesa DJ, Buswinka CJ, Rabah AM, Swiderski DL, Raphael Y, Pfingst BE 2020. How electrically evoked compound action potentials in chronically-implanted guinea pigs relate to auditory nerve health and electrode impedance. J. Acoust. Soc. Amer. 148, 3900–3912. doi: 10.1121/10.0002882. [PubMed: 33379919]

Schvartz-Leyzac KC, Colesa DJ, Buswinka CJ, Swiderski DL, Raphael Y, Pfingst BE 2019. Changes over time in the electrically evoked compound action potential (ECAP) interphase gap (IPG) effect following cochlear implantation in guinea pigs. Hear Res 383, 107809. doi: 10.1016/j.heares.2019.107809. [PubMed: 31630082]

Schvartz-Leyzac KC, Pfingst BE 2018. Assessing the relationship between the electrically evoked compound action potential and speech recognition abilities in bilateral cochlear implant recipients. Ear Hear 39, 344–358. doi:10.1097/AUD.0000000000000490. [PubMed: 28885234]

Searchfield GD, Munoz DJ, Thorne PR 2004. Ensemble spontaneous activity in the guinea-pig cochlear nerve. Hear Res 192, 23–35. doi:10.1016/j.heares.2004.02.006. [PubMed: 15157960]

Smith L, Simmons FB 1983. Estimating eighth nerve survival by electrical stimulation. Ann Otol Rhinol Laryngol 92, 19–23. doi:10.1177/000348948309200105. [PubMed: 6824273]

Soken H, Robinson BK, Goodman SS, Abbas PJ, Hansen MR, Kopelovich JC 2013. Mouse cochleostomy: A minimally invasive dorsal approach for modeling cochlear implantation. Laryngoscope 123, E109–15. doi:10.1002/lary.24174. [PubMed: 23674233]

Su GL, Colesa DJ, Pfingst BE 2008. Effects of deafening and cochlear implantation procedures on postimplantation psychophysical electrical detection thresholds. Hear Res 241,64–72. doi:10.1016/j.heares.2008.04.011. [PubMed: 18558467]

Swiderski DL, Colesa DJ, Hughes AP, Raphael Y, Pfingst BE 2020. Relationships between intrascalar tissue, neuron survival, and cochlear implant function. J Assoc Res Otolaryngol 21,337–352. doi:10.1007/s10162-020-00761-4. [PubMed: 32691251]

Tong L, Strong MK, Kaur T, Juiz JM, Oesterle EC, Hume C, Warchol ME, Palmiter RD, Rubel EW 2015. Selective deletion of cochlear hair cells causes rapid age-dependent changes in spiral ganglion and cochlear nucleus neurons. J Neurosci 35, 7878–91. doi:10.1523/JNEUROSCI.2179-14.2015. [PubMed: 25995473]

Wilk M, Hessler R, Mugridge K, Jolly C, Fehr M, Lenarz T, Scheper V 2016. Impedance Changes and fibrous tissue growth after cochlear implantation are correlated and can be reduced using a dexamethasone eluting electrode. PloS One 11, e0147552. doi: 10.1371/journal.pone.0147552. [PubMed: 26840740]

Highlights

- Cochlear implant function in mice should be assessed in the awake state
- Implantation in mice can cause some hair cell and auditory neuron loss
- ECAP AGF Slopes are safe and effective for assessment of cochlear health in mice
- ECAP AGF Slopes often improve over time after implant insertion
- Data from mice with chronic cochlear implants are similar to those from guinea pigs

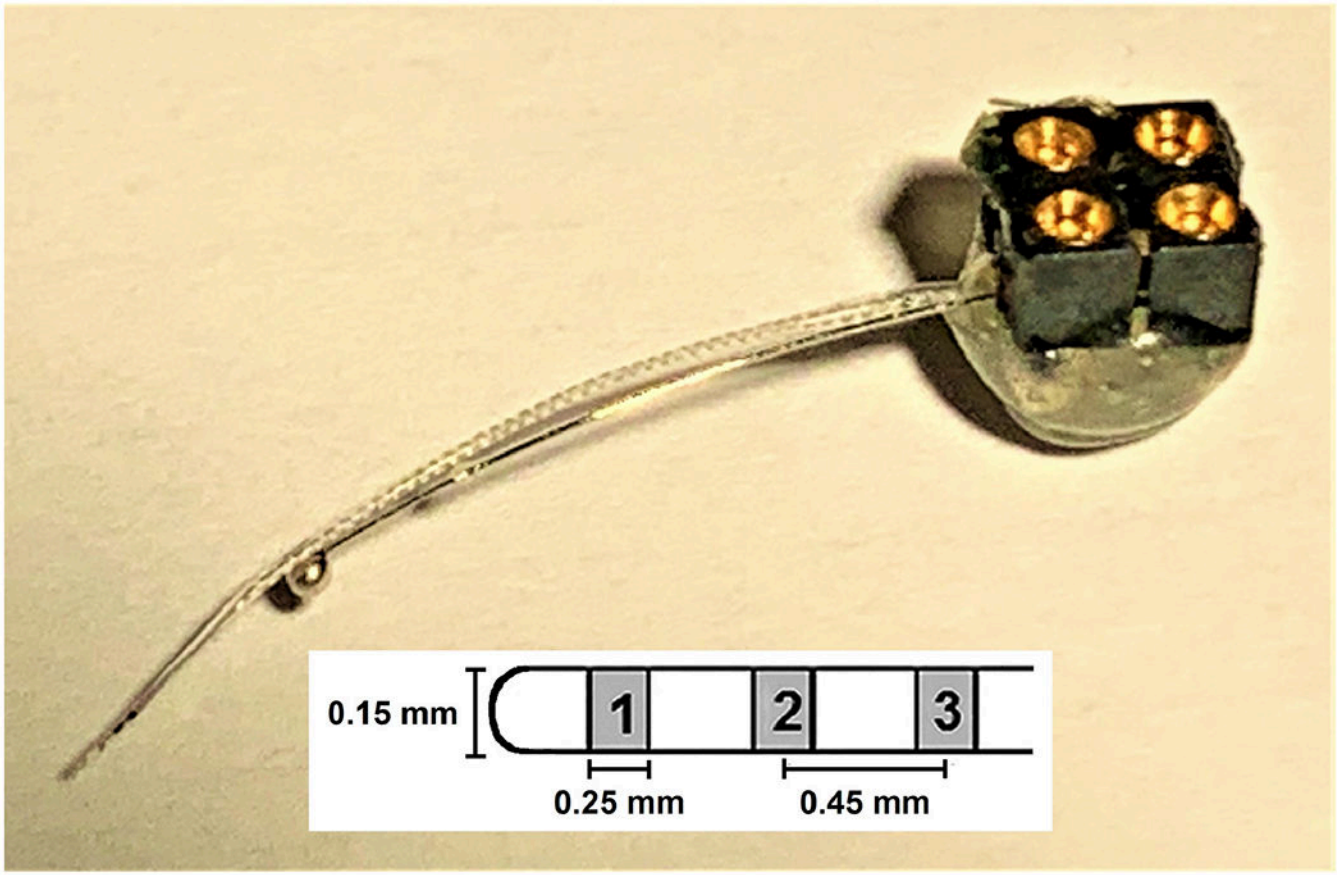

Figure 1.

Mouse multichannel cochlear implant. Three half-band platinum/iridium electrodes (~ 0.25 mm) mounted on a silastic carrier (see diagram) served as the intracochlear stimulating/recording electrodes. These three-electrode arrays were purchased from Cochlear®. The large ball electrode (~ 0.8 mm diameter), made in house, served as the ground electrode for stimulation and recording. The intracochlear electrodes were labeled 1 through 3, with 1 being the most apically inserted electrode and the primary electrode used for centering the histology sections. The electrodes were hard-wired to a four-contact percutaneous connector (Samtec) that was mounted on the animal's skull.

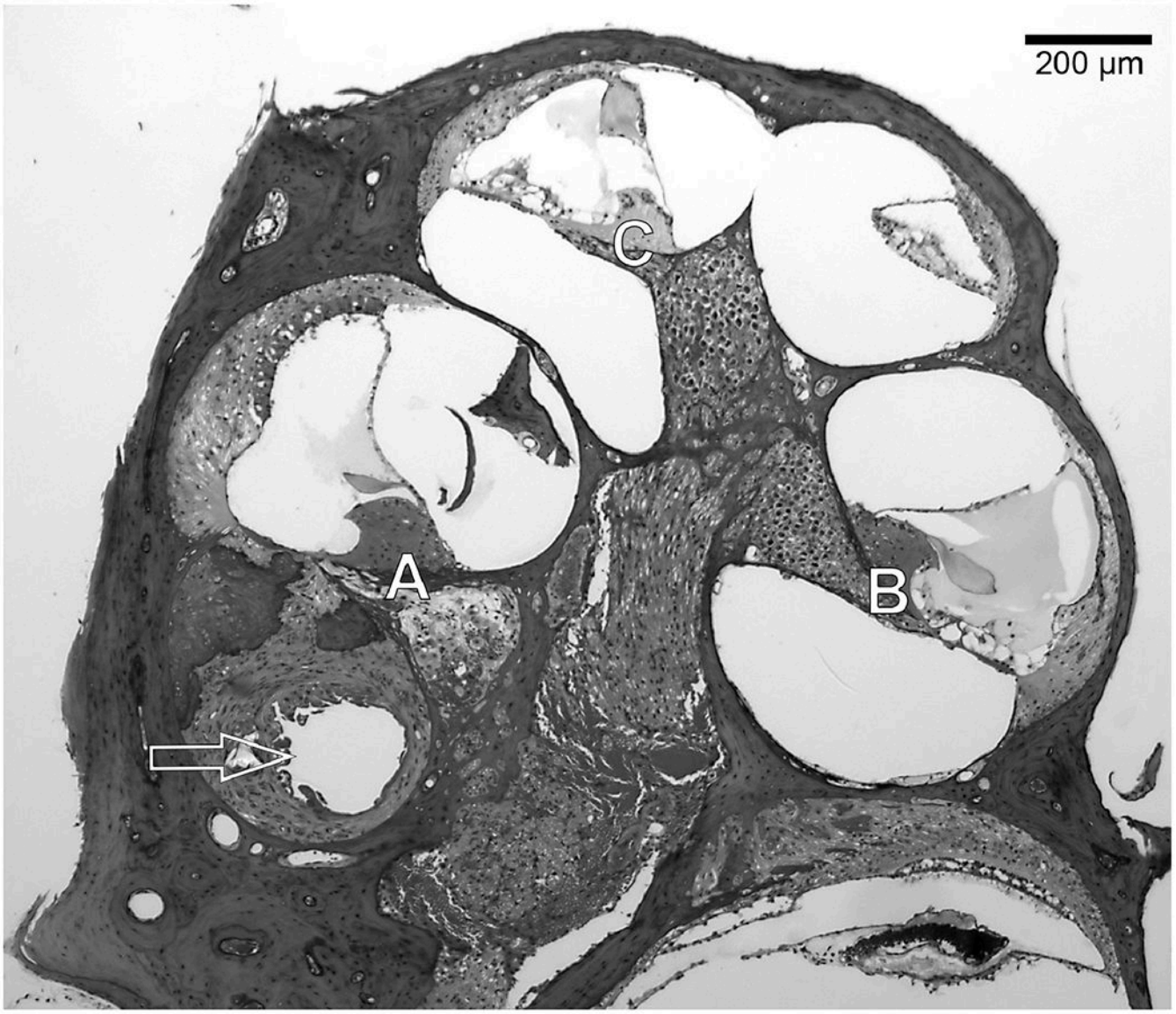

Figure 2.

Mid-modiolar section of a mouse cochlea showing the Profiles A through C that were the regions examined for SGN and IHC survival. Sections were taken in the area of electrode 1. The arrow shows the location of the implant footprint in the fibrous tissue and new bone that had surrounded the implant.

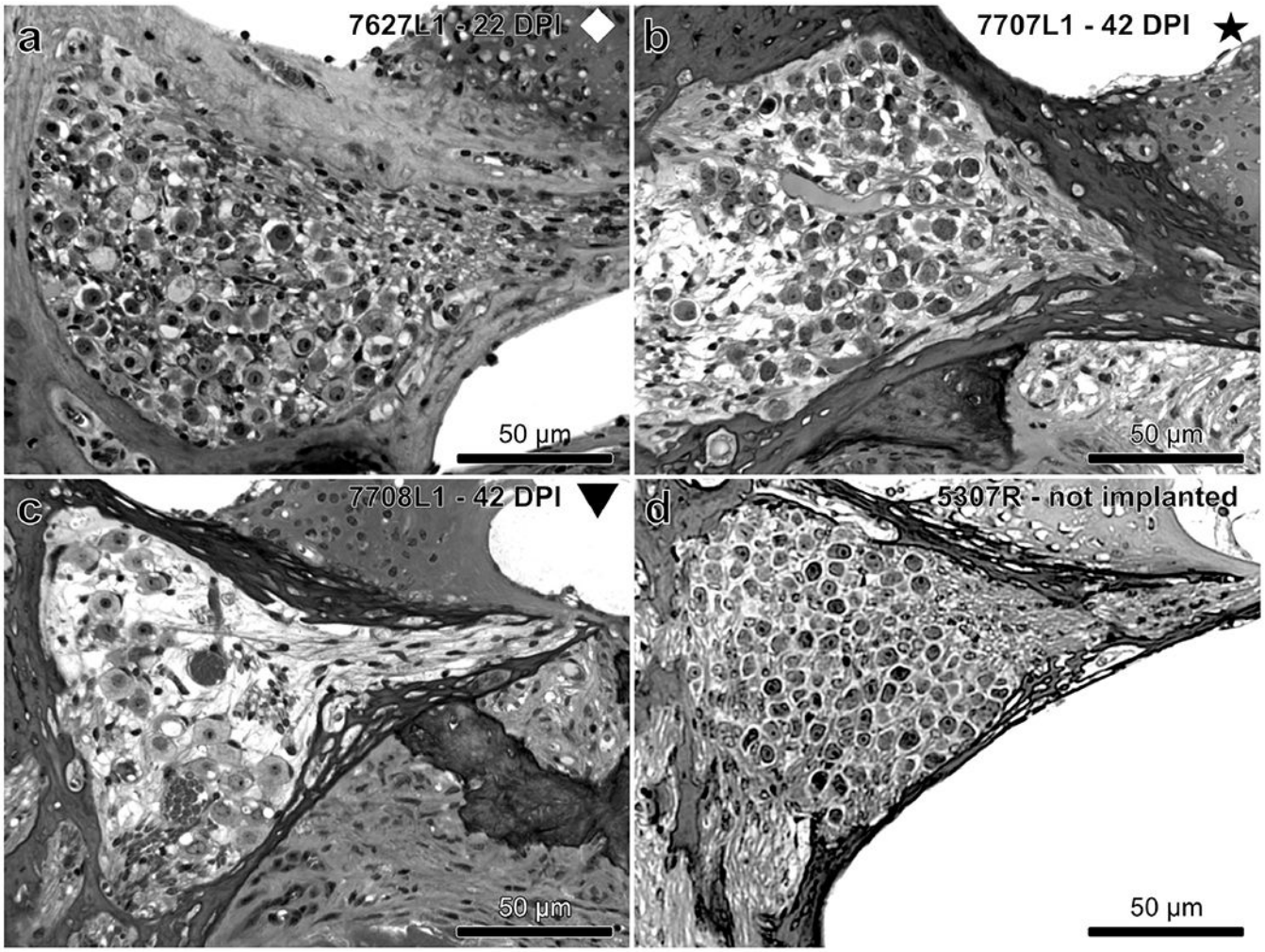

Figure 3.

Examples of the variability seen in SGN density in Rosenthal's canal of mice with a multichannel cochlear implant (a – c) compared to a normal non-implanted mouse (d) taken from Profile A. SGN density appears high (a), medium (b) or low (c). Intrascalar tissue (fibrosis and bone; partially seen) is absent in (a) but present in (b) and (c). Symbols indicate the identities of the mice throughout the manuscript.

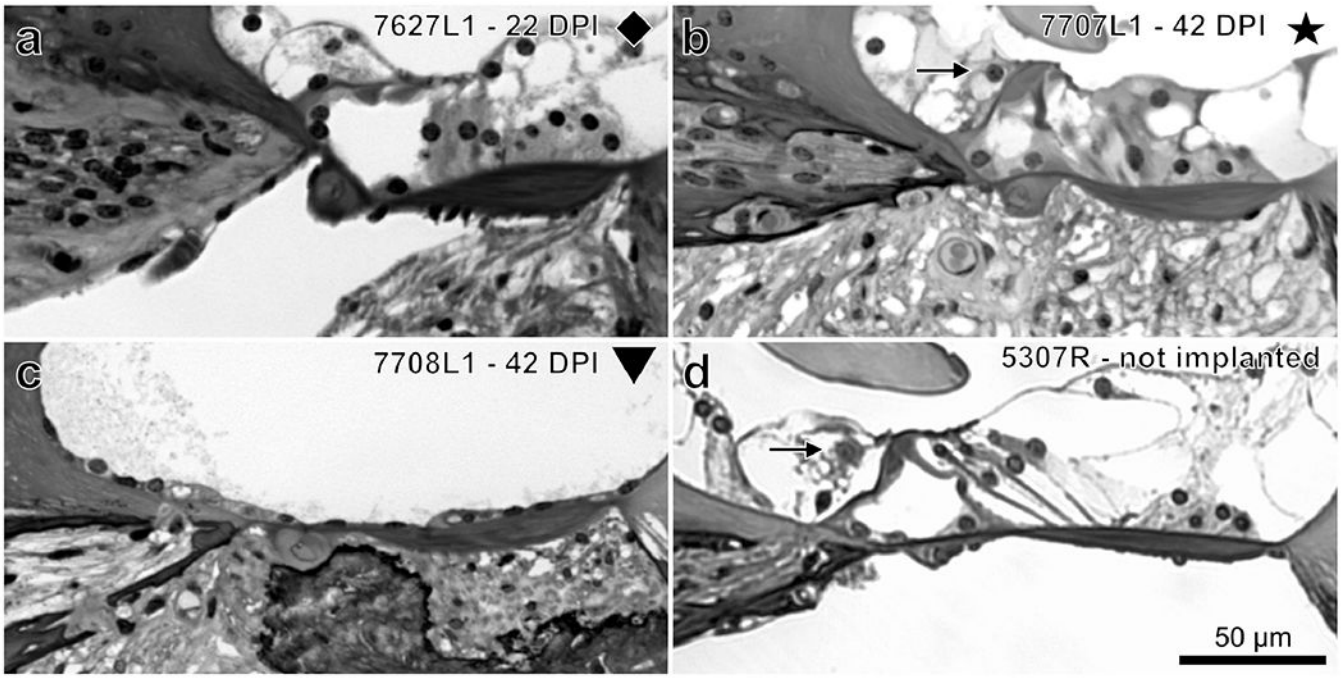

Figure 4.

Examples of the variability seen in IHC and supporting cell survival in the organ of Corti of mice with a multichannel cochlear implant (a, b, c) compared to a normal non-implanted mouse (d) in Profile A. (a) IHCs are absent but supporting cells survive. (b) Both IHCs (arrow) and supporting cells are present. (c) The organ of Corti was replaced by a flat epithelium with no IHC or supporting cells. (d) Normal organ of Corti.

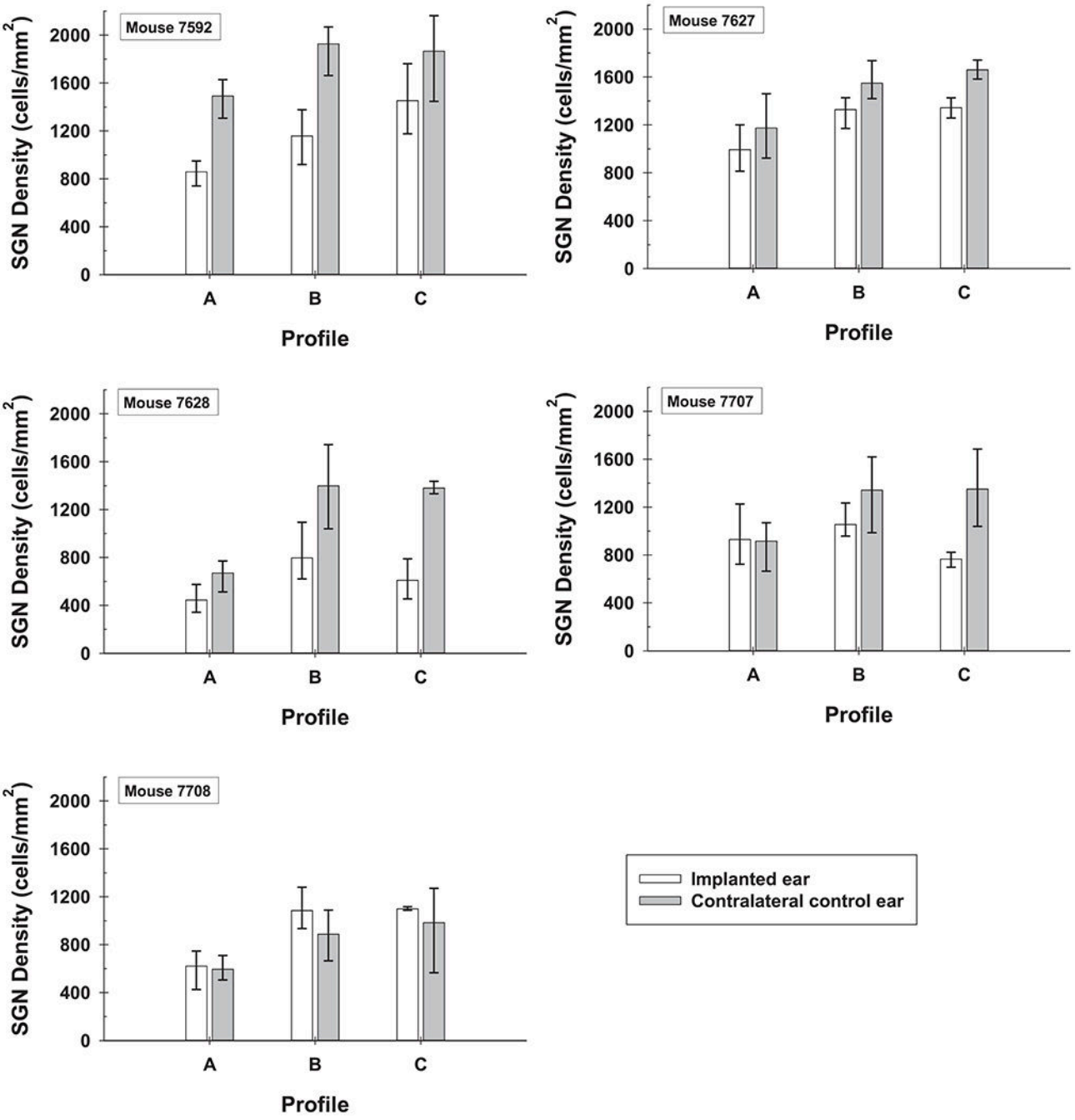

Figure 5.

Comparison of SGN density throughout the cochlea (Profiles A through C) for implanted and non-implanted ears of all five mice. Error bars are the range of SGN densities (maximum to minimum) for the 3 histological sections analyzed per ear.

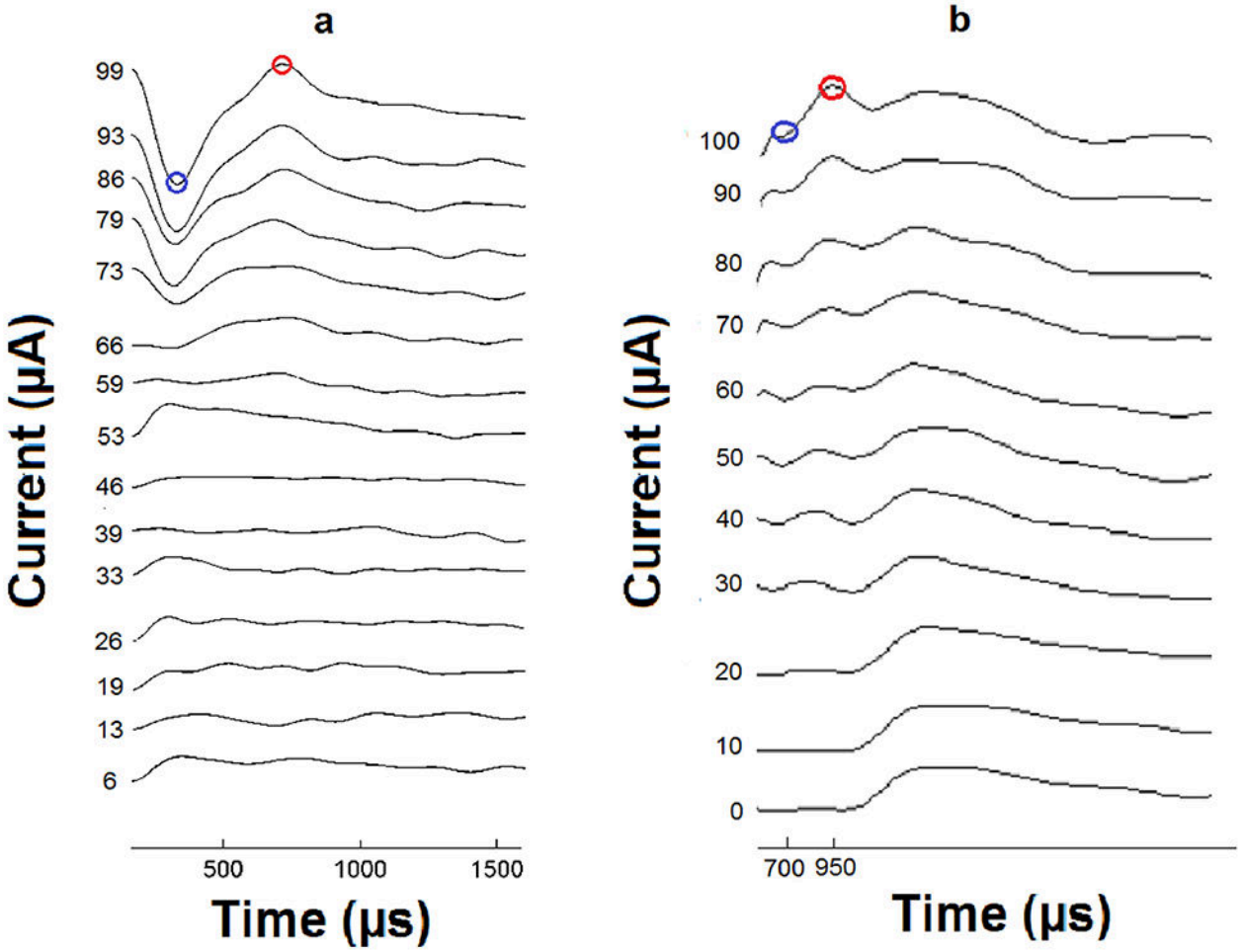

Figure 6.

Examples of an ECAP (a) and EABR (b) recording (electrical responses to stimuli recorded from the auditory nerve and brainstem, increasing with stimulus strength). N1 peaks are labeled in blue circles and P2 peaks are labeled in red circles. The N1 to P2 amplitudes in μV were plotted against stimulus current in μA to obtain input-output amplitude-growth functions. (a) For the ECAP recordings all peaks were selected by an automated custom program. When calculating slope of the ECAP AGFs, a linear regression was applied to fit all data points from 100 μV to the MSL, providing that the ECAP amplitudes continued to increase as a function of level. (b) For EABR recordings, all peaks were manually selected. When calculating slope of the AGFs for EABR, a linear regression was applied to fit all data points from 0.25 μV to the MSL, providing that the EABR amplitudes continued to increase as a function of level.

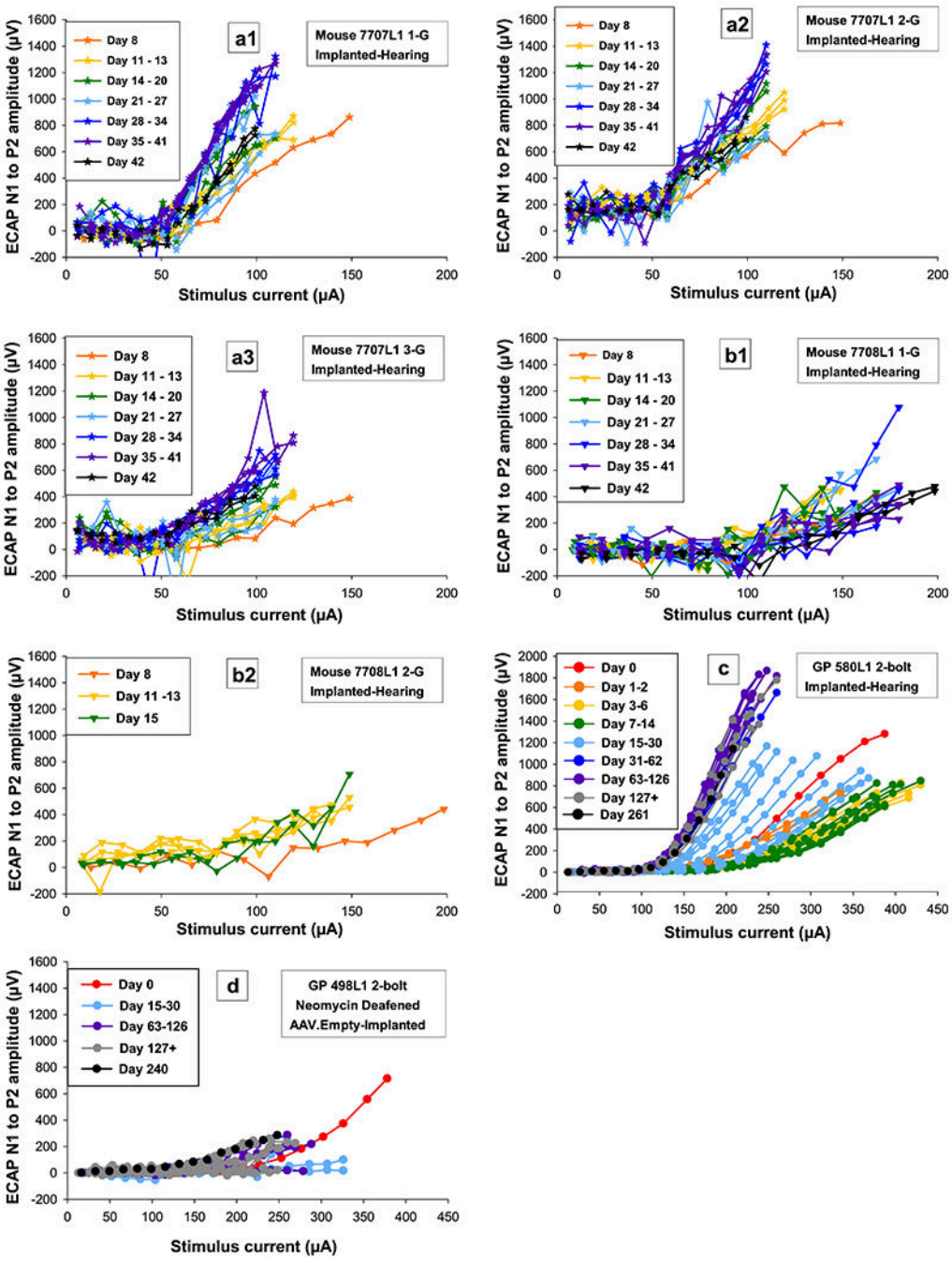

Figure 7.

Electrically-evoked compound action potential (ECAP) amplitude-growth functions (AGFs; electrical responses to stimuli recorded from the auditory nerve, increasing with stimulus strength) over time for two mice (a and b) for multiple electrodes that were tested up to 42 DPI and two guinea pigs, one with good cochlear health tested up to 261 DPI (c) and one with poor cochlear health tested up to 240 DPI (d). Recovery in AGFs over time can be seen for mouse 7707L1 for all tested electrodes (a1, 2, and 3) and the guinea pig with good cochlear health (c). For mouse 7708L1 (b1 and 2) and the guinea pig with poorer cochlear

health (d), AGFs recover less or not at all over time. Individual symbols are specified for each mouse and circles for guinea pigs. Color progressions show changes over time with all final data points in black regardless of DPI. For further information, identification boxes list the species, animal number, stimulating electrode condition (i.e. 1-G means electrode 1 was being stimulated and its return ground was G the ball in the neck), and treatment paradigm.

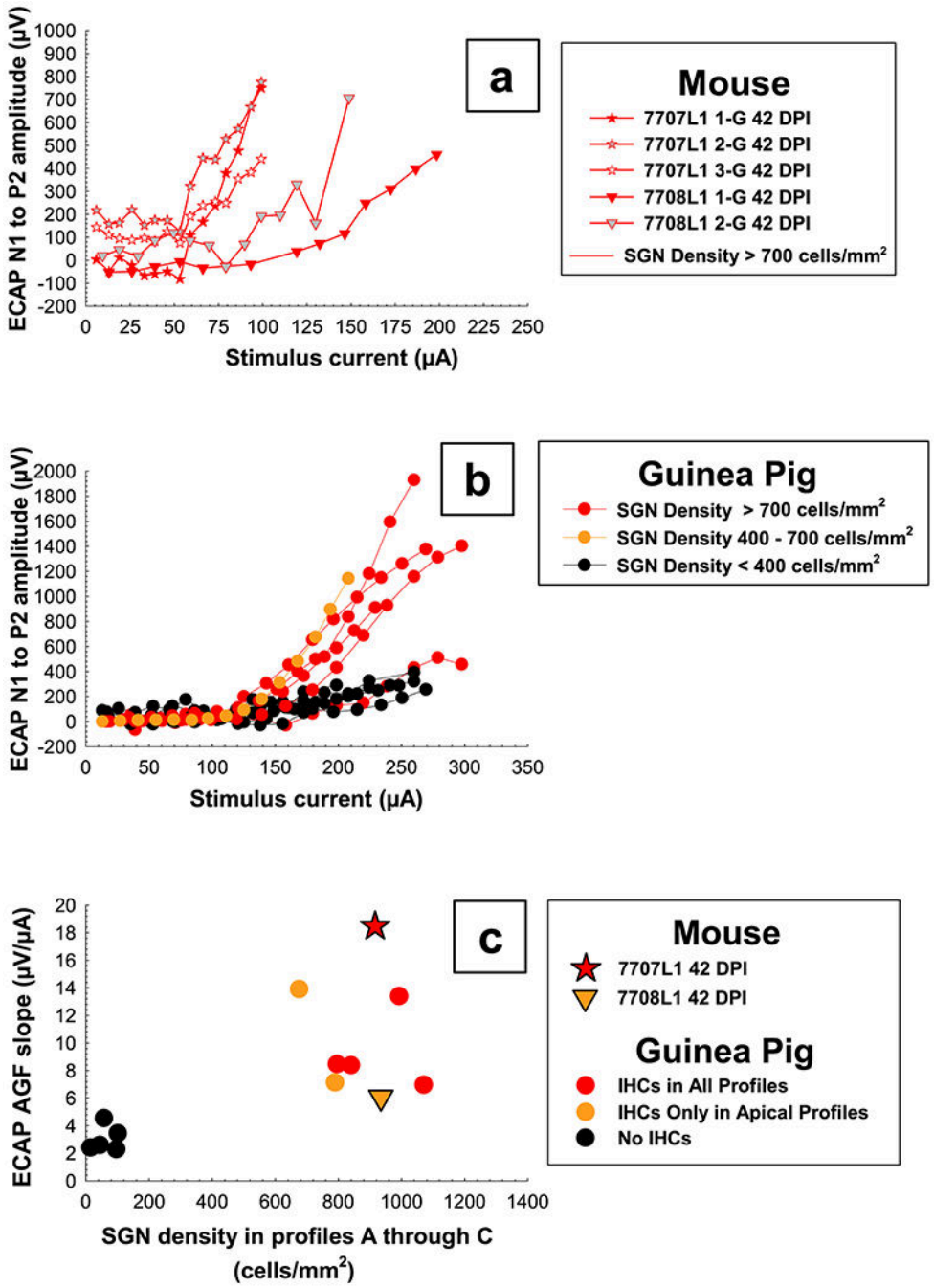

Figure 8.

ECAP AGFs on the final day tested for all electrodes for two mice (top panel, a) and the primary electrode for multiple guinea pigs of varying cochlear health (middle panel, b). AGF slopes for the primary electrode have been plotted as a function of average SGN density for histology Profiles A through C (bottom panel, c) to show how these two mice have similar slopes to guinea pigs of comparable cochlear health; slope for guinea pigs with good cochlear health can range from around 6 - 22 μV/μA (the guinea pig setting the upper value for this range is still being tested and therefore not shown here). Slopes for each mouse

represent the average slope of the two growth functions measured on 42 DPI for electrode 1 and slopes for each guinea pig represent the mean slopes of multiple growth functions obtained during a period when slopes were relatively stable over time (150 DPI to euthanasia) for the primary electrode. Individual symbols are specified for each mouse and circles for guinea pigs. Colors were coded by SGN for panels a and b and IHC survival in Profiles A through C for panel c; red = high, yellow = medium to low, and black = low SGN and no IHC survival.

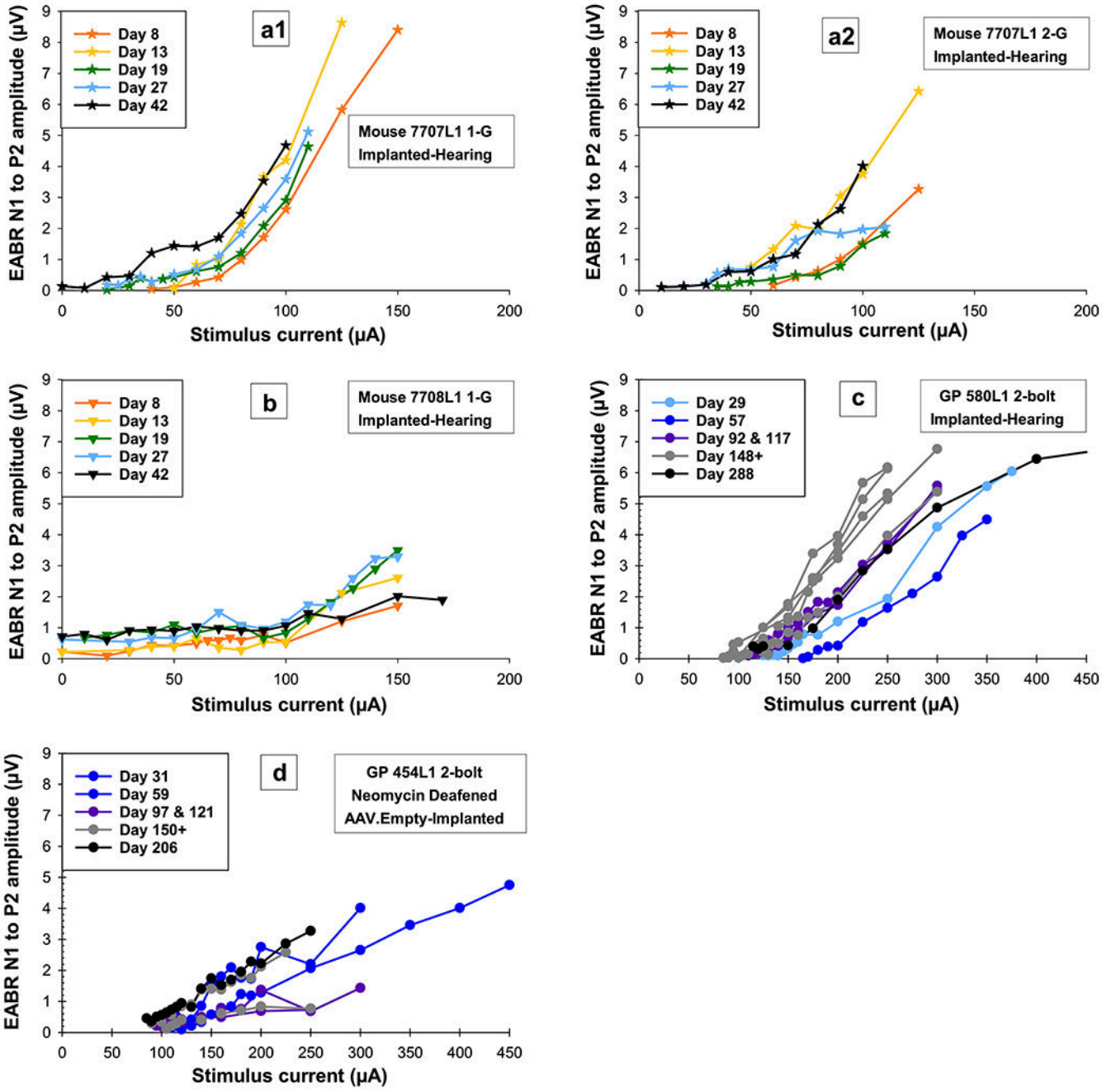

Figure 9.

Electrically-evoked auditory brainstem response (EABR) amplitude-growth functions (AGFs, electrical responses to stimuli recorded from the brainstem, increasing with stimulus strength) over time for two mice (a and b) for multiple electrodes that were tested up to 42 DPI and two guinea pigs, one with good cochlear health tested up to 288 DPI (c) and one with poor cochlear health tested up to 206 DPI (d). Similar to the ECAP, recovery in EABR AGFs over time can be seen for mouse 7707L1 for all tested electrodes (a1 and 2) and the guinea pig with good cochlear health (c). For mouse 7708L1 (b) and the guinea pig with poorer cochlear health (d), AGFs recover less or not at all over time. Individual symbols are

specified for each mouse and circles for guinea pigs. Color progressions show changes over time with all final data points in black regardless of DPI. For further information, identification boxes list the species, animal number, stimulating electrode condition (i.e. 1-G means electrode 1 was being stimulated and its return ground was G the ball in the neck), and treatment paradigm.

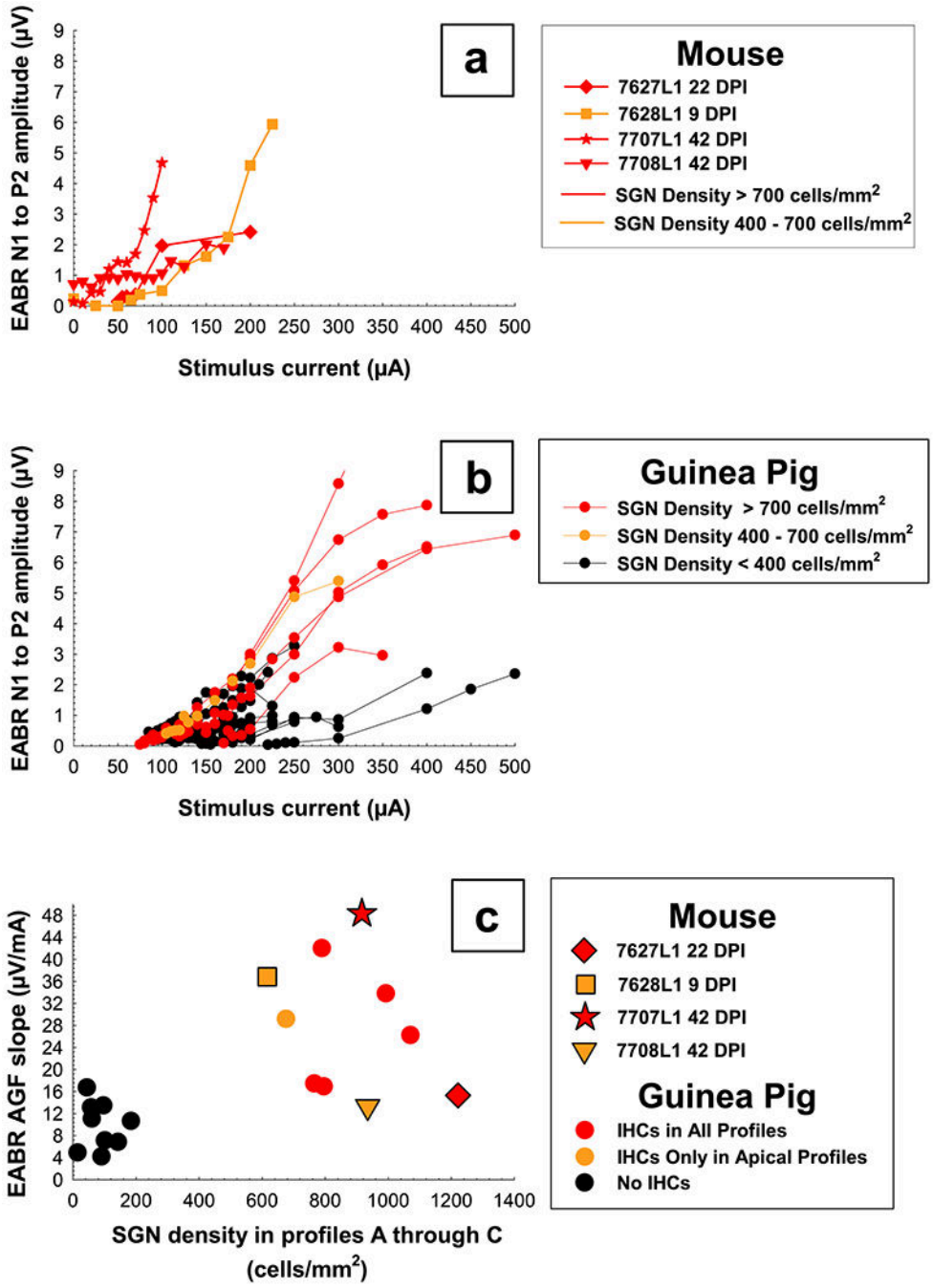

Figure 10.

EABR AGFs for four mice (top panel, a) and guinea pigs of varying cochlear health (middle panel, b) for the primary electrode on the final day tested. AGF slopes have been plotted as a function of average SGN density for histology Profiles A through C (bottom panel, c) to show how these four mice have similar slopes to guinea pigs of comparable cochlear health. Slopes for each mouse represent one growth function obtained on the last day usable data was collected and slopes for each guinea pig represent the average slope of multiple growth functions obtained during a period when slopes were relatively stable over time (150 DPI to

euthanasia). Individual symbols are specified for each mouse and circles for guinea pigs. Colors were coded by IHC survival in Profiles A through C; red = high, yellow = medium to low, and black = no IHC survival.

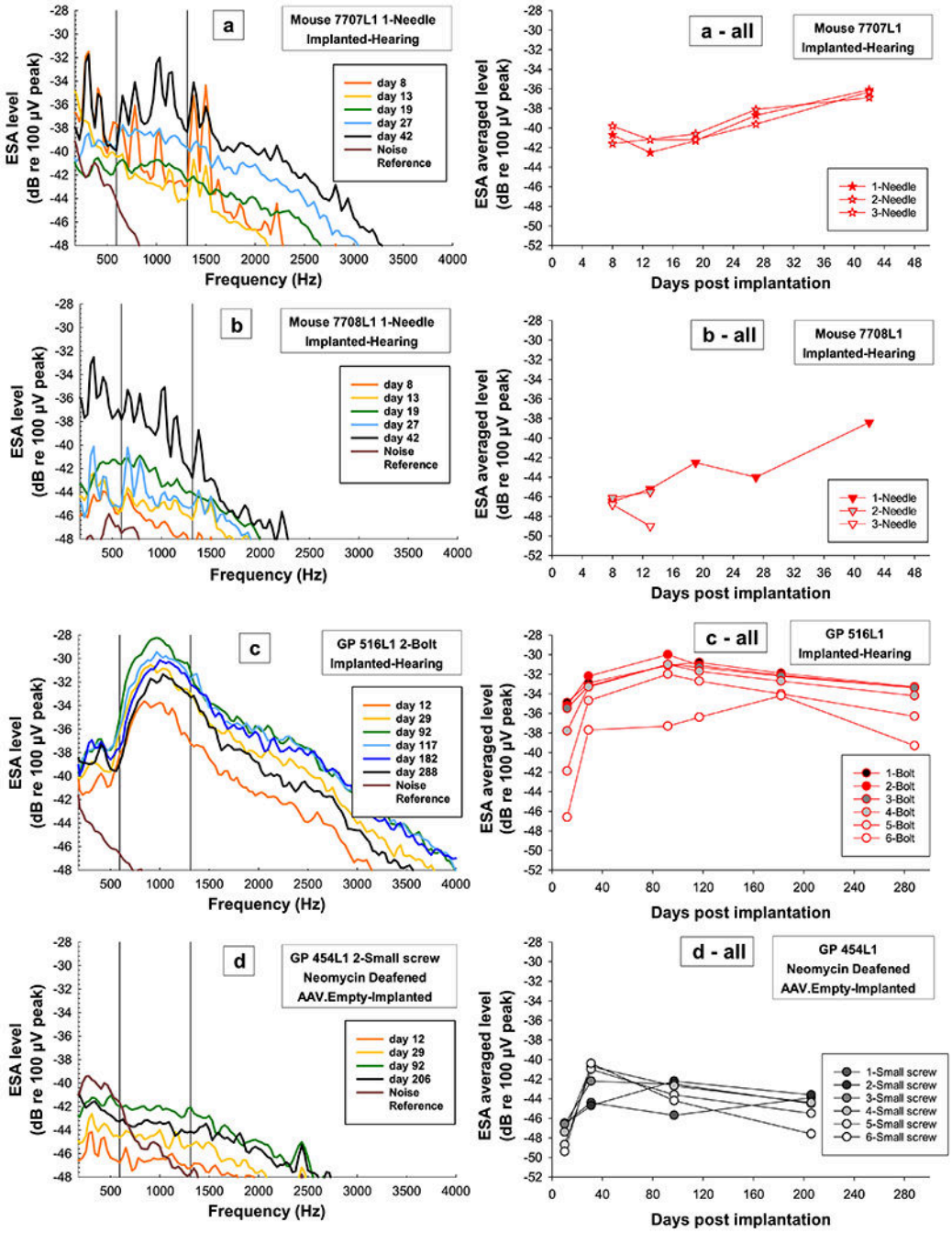

Figure 11.

ESA spectra examples (left column) from the primary electrode and average ESA levels over time for all electrodes (right column) for two mice (a and b) that were tested up to 42 DPI and two guinea pigs, one with good cochlear health tested up to 288 DPI (c) and one with poor cochlear health tested up to 206 DPI (d). ESA spectra (left column) reflect the spontaneous activity in the auditory nerve and for all animals and treatment groups (a, b, c, and d) show how spontaneous activity recovers and increases in level over time after surgery. ESA spectra are for the primary electrode to ground (needle, bolt, small screw); grounds

from the mice were needles and for the guinea pigs either the bolt or small screw if the bolt was not making good contact). Color progressions on the spectra show changes over time with all final data points in black regardless of DPI; brown lines show the ambient noise in the system. Black vertical lines represent the frequency range (593.75-1312.5 Hz) in which a "normal" ESA level would occur in guinea pigs if hair cells were present. ESA levels were averaged over this frequency range to make it possible to compare animals with the peak (a, b and c) to animals without the peak (d) and to give a metric for presence and absence of IHCs and spontaneous activity levels. These ESA averaged levels over time are plotted (right column) to show how spontaneous activity increases with time after surgery (DPI) regardless of species, treatment group or electrode location; mice were still increasing up to 42 DPI and guinea pigs increased and then showed long-term stable trends. ESA averaged levels are for all electrodes and were coded by individual symbols for each mouse and circles for guinea pigs; colors were coded by IHC survival in Profiles A through C; red = high, yellow = medium to low, and black = no IHC survival).

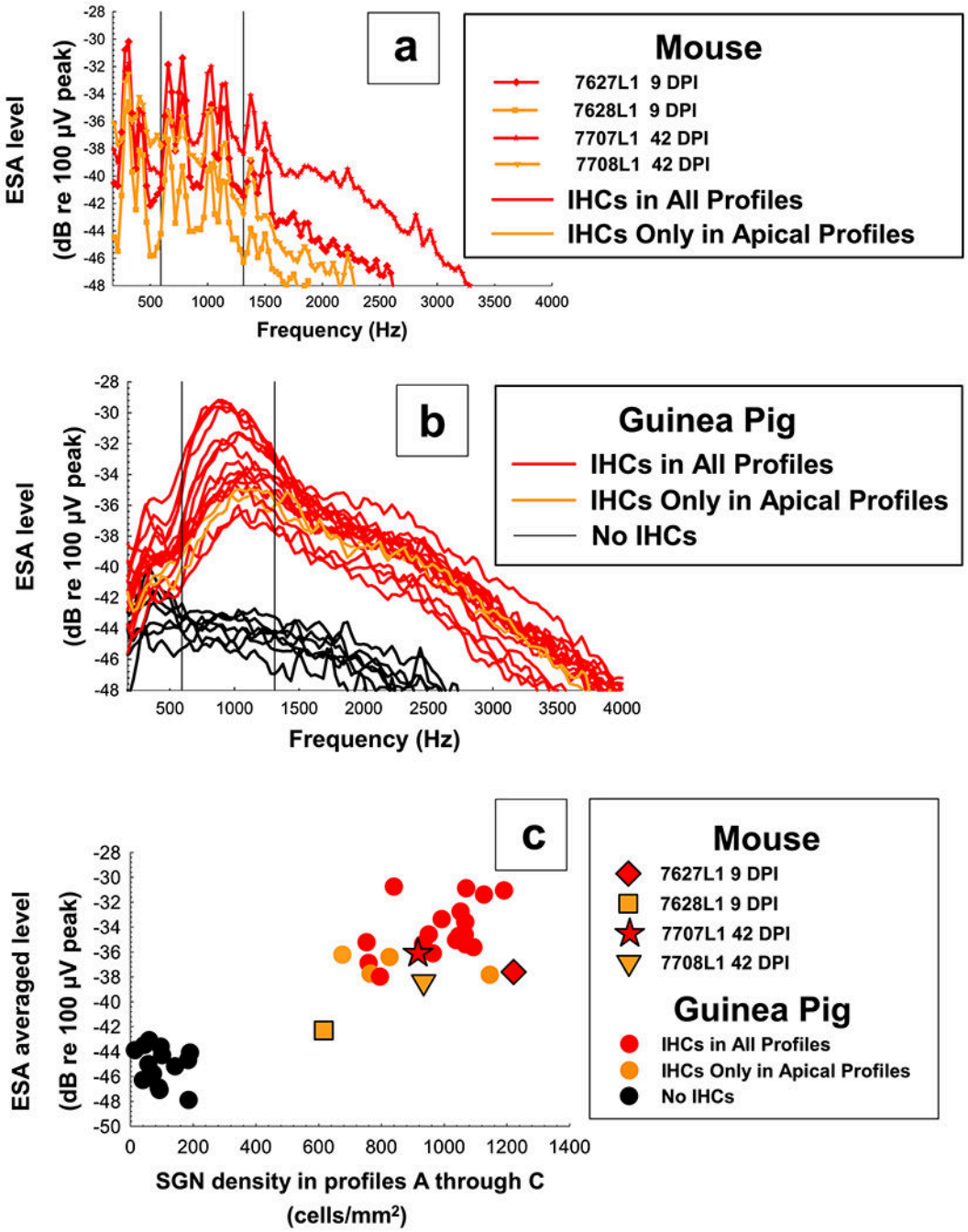

Figure 12.

ESA spectra for mice (top panel, a) and guinea pigs of varying cochlear health (middle panel, b) on the final day tested. ESA averaged levels of these spectra have been plotted as a function of average SGN density for histology Profiles A through C (bottom panel, c) to show how these four mice have similar average ESA levels to guinea pigs of comparable cochlear health. ESA levels for each mouse and guinea pig represent one representative spectra obtained on the last day usable data was collected. Individual symbols are specified

for each mouse and circles for guinea pigs. Colors were coded by IHC survival in Profiles A through C; red = high, yellow = medium to low, and black = no IHC survival.

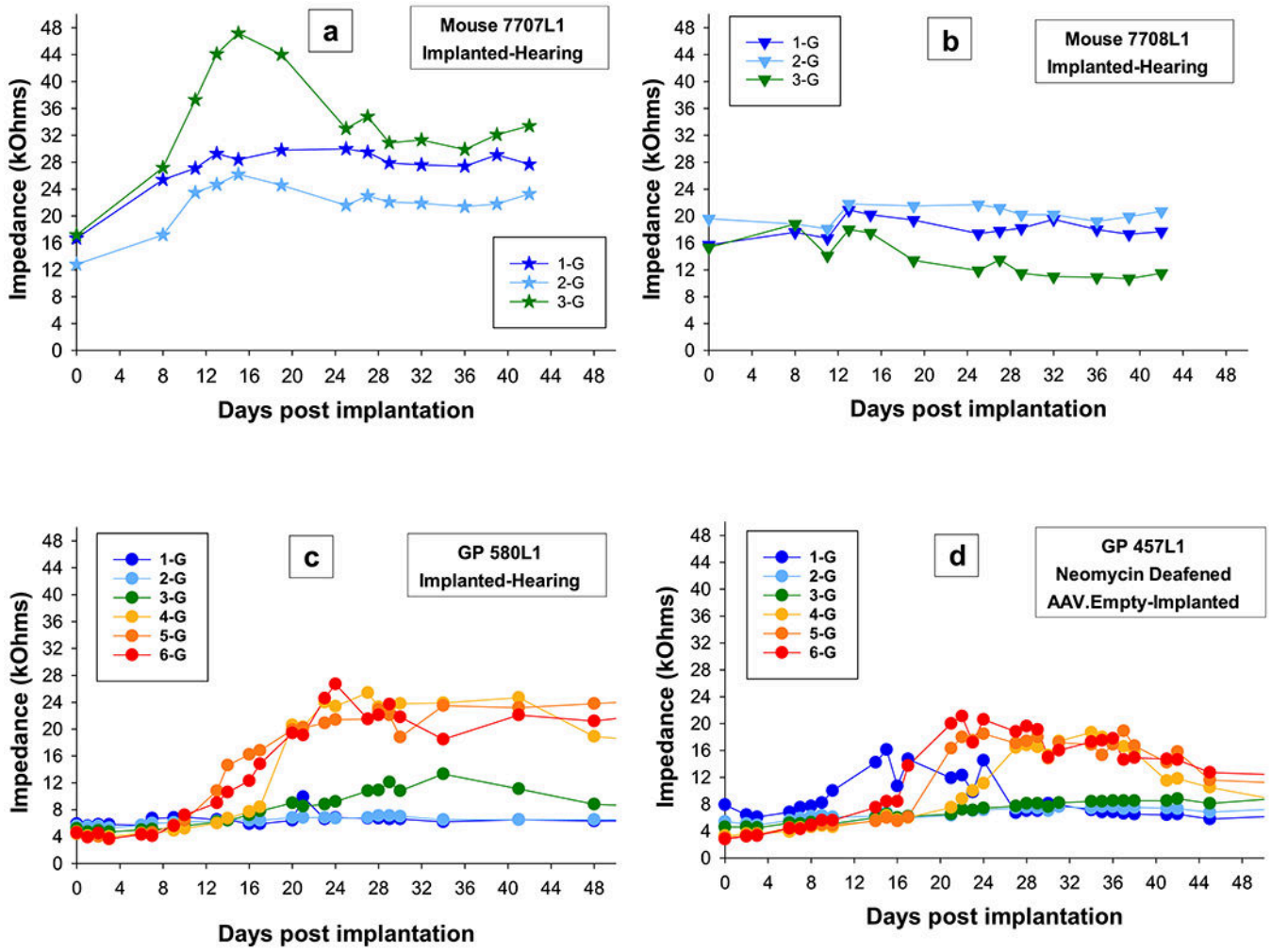

Figure 13.

Impedances over time for all electrodes for the two mice (a and b) that were tested up to 42 DPI and two guinea pigs, one with good cochlear health (c) and one with poor cochlear health (d). Impedances in mice and guinea pigs were similar in changes over time with impedances for individual electrodes showing one of four trends: 1) impedances that have a gradual increase and then stabilize, 2) impedances that show a gradual increase and then decrease to a steady state, 3) impedances that have a decrease to a steady state, and 4) impedances that show no change. Individual symbols are specified for each mouse and circles for guinea pigs. Colors progress from blue to red and represent the apical to basal electrodes.

Table 1.

Summary of histology, electrophysiology, ESA and impedance results for the implanted left ear of all mice. Functional data trends are only for electrode 1 where the histology was taken.

Mouse #, Ear, and Implant #		7592L1	7627L1	7628L1	7707L1	7708L1
Age at Implantation (months)	Profile ↓	1.5	1.8	1.8	1.8	1.8
Duration of implantation (days)		29	22	16	46	42
SGN Density and Range (cells/mm^2	A	858 (741 – 949)	993 (814 – 1200)	444 (342 – 575)	928 (723 – 1227)	621 (426 – 747)
	B	1158 (920 – 1377)	1327 (1171 – 1427)	796 (621 – 1095)	1054 (957 – 1235)	1084 (935 – 1279)
	C	1452 (1176 – 1761)	1343 (1257 –1426)	609 (454 – 788)	765 (697 – 822)	1098 (1087 – 1117)
Average SGN Density (cells/mm^2)	A-C	1187	1214	616	950	939
IHC Survival	A	high	medium	high	medium	absent
	B	high	high	low	high	medium
	C	medium	high	absent	medium	high
Average IHC Survival	A-C	high	high	low	medium	medium
Intrascalar Tissue	A	high density	low density	high density	high density	high density
	B	high density	absent	high density	absent	absent
	C	absent	absent	absent	absent	absent
ECAP Slope; Pattern Over Time		NA	NA	NA	Steep; Increasing to a plateau	Shallow; Stable and shallow from the start
EABR Slope; Pattern Over Time		NA	Shallow; NA	Steep; NA	Steep; Increasing then decreasing	Shallow; Increasing then decreasing
ESA Present; Pattern Over Time		NA	Large peak; NA	Small peak; NA	Large peak; Increasing	Medium peak; Increasing
Impedance		Off scale after 15 DPI	Off scale after 16 DPI	Off scale after day 9 testing	Increasing to day 15, then stable to 42 DPI	Stable from start to 42 DPI